The environmental and geomorphological impacts of historical gold mining in the Ohinemuri and Waihou river catchments, Coromandel, New Zealand

Alastair J.H. Clement[1*], Tereza Nováková[2,3], Karen A. Hudson-Edwards[4], Ian C. Fuller[1,5], Mark G. Macklin[5,6], Elizabeth G. Fox[1], Ignacio Zapico[7]

1 Physical Geography Group, Institute of Agriculture and Environment, Massey University, Private Bag 11-222, Palmerston North 4442, New Zealand

2 Institute of Inorganic Chemistry AS CR, v.v.i., Husinec-Rez 1001, 250 68 Rez, Czech Republic

3 Institute of Geology of the CAS, v. v. i., Rozvojova 269, 165 00, Prague, Czech Republic

4 Department of Earth and Planetary Sciences, Birkbeck, University of London, Malet St., London WC1E 7HX, UK

5 Innovative River Solutions, Institute of Agriculture and Environment, Massey University, Private Bag 11-222, Palmerston North 4442, New Zealand

6 School of Geography and the Lincoln Centre for Water and Planetary Health, University of Lincoln, LN6 7TS Lincoln, UK

7 Facultad de Ciencias Geológicas, José Antonio Novais, 12, Ciudad Universitaria, 28040 Madrid, Spain

* Corresponding author: Tel: +64 6 951 7847; Email: a.clement@massey.ac.nz

Abstract

Between 1875 and 1955 approximately 250,000 Mg yr^{-1} of mercury-, arsenic-, and cyanide-contaminated mine tailings were discharged directly into the Ohinemuri River and its tributaries, in the Coromandel Region, North Island, New Zealand. A devastating flood on 14 January 1907 deposited large amounts of mine waste across the floodplain of the Ohinemuri and Waihou rivers in the vicinity of the township of Paeroa. The 1907 mine-waste flood deposit was located as a dirty yellow silt in cores and floodplain profiles, with a thickness ranging from 0.15-0.50 m. Geochemical analysis of the mine waste shows elevated concentrations of Pb (~200-570 mg kg^{-1}) and As (~30-80 mg kg^{-1}), compared to early Holocene background concentrations (Pb <30 mg kg^{-1}; As <17 mg kg^{-1}). Bulk sediment samples recovered from the river channel and overbank deposits also show elevated concentrations of Pb (~110 mg kg^{-1}), Zn (~140-320 mg kg^{-1}), Ag (~3 mg kg^{-1}), and Hg (~0.4 mg kg^{-1}). Using the mine-waste deposit as a chronological marker shows that sedimentation rates increased from ~0.2 mm yr^{-1} in the early Holocene, to 5.5-26.8 mm yr^{-1} following the 1907 flood. Downstream trends in the thickness of the flood deposit show that local-scale geomorphic factors are a significant influence on the deposition of mine waste in such events. Storage of mine waste is greatest in the upstream reaches of the floodplain. The volume of mine waste estimated to be stored in the Ohinemuri floodplain is ~1.13 M m^3, an order of magnitude larger than recent well-publicised tailings-dam failures, such as the 1996 South America Porco, 2000 Romanian Baia Mare and Baia Borsa accidents, and constituted, and was recognised at the time, a significant geomorphological and environmental event. The mine-waste material remains in the floodplain today, representing a sizable legacy store of contaminant metals and metalloids that pose a long-term risk to the Ohinemuri and Waihou ecosystems.

48

49 **Highlights**

50 • A January 1907 flood dispersed gold mining tailings in the
51 Ohinemuri/Waihou rivers

52 • ~1.13 M m^3 of tailings from this event is stored in the Ohinemuri/Waihou
53 floodplains

54 • Sedimentation rates increased by an order of magnitude following the
55 1907 flood

56 • Contaminant metals and metalloids pose a long-term risk to the
57 ecosystem

58 • The environmental legacy of historical mining must be considered in river
59 management

60 **Keywords**

61 Mining-contaminated river; floodplain sedimentation; mine tailing discharge;
62 historical gold mining; Ohinemuri River; Waihou River

63

64 **1. Introduction**

65 Historical metal mining activities routinely disposed of large quantities of mine
66 tailings directly into streams and rivers (e.g., Lewin and Macklin, 1987; Salomons,
67 1995; Black et al., 2004; Macklin et al., 2006). As a result, river systems in many
68 parts of the world were contaminated by metal-rich wastes in hazardous
69 concentrations (e.g., Macklin et al., 2006 and references therein). River

floodplains function as semi-permanent sinks for these metal contaminants (Bradley, 1989; Moore and Luoma, 1990; Lecce and Pavlowsky, 1997; Black et al., 2004), with the residence time of metal contaminants within the fluvial system regulated by the system's sediment storage capacity (Bradley, 1989; Macklin et al., 1994; Macklin, 1996; Lecce and Pavlowsky, 1997; Black et al., 2004), sediment transport processes (Lewin et al., 1977; Lewin and Wolfenden, 1978; Bradley, 1984; Lewin and Macklin, 1987; Marcus, 1987; Graf, 1990; Axtmann and Luoma, 1991; Walling et al., 2003; Taylor and Kesterton, 2002), flooding regime (Leenaers, 1989; Macklin and Dowsett, 1989; Miller et al., 1999; Ciszewski, 2001; Marcus et al., 2001; Dennis et al., 2003), and the rate and manner of mine waste disposal during the period of historical mining activity (Bradley, 1989; Rang and Schouten, 1989; Bradley and Cox, 1990; Macklin and Klimek, 1992; Lecce and Pavlowsky, 1997; Macklin et al., 2002). The present-day hazard posed by metal-mining contaminants in floodplain sediments is therefore the product of these geomorphic controls on residence time coupled with contemporary rates of chemical weathering and fluvial erosion of tailings deposits.

The contamination legacy of historical metal mining has been investigated in Europe (Lewin and Macklin, 1987; Bradley, 1989; Macklin, 1992; Passmore and Macklin, 1994; Hudson-Edwards et al., 1998; Macklin et al., 2006; Bird et al., 2008, 2010; Macklin et al., 2014), the USA (Lecce and Pavlowsky, 1997; Miller, 1997; Miller et al., 1999; James, 2013), and South America (Hudson-Edwards et al., 2001; Miller et al., 2002). In New Zealand the majority of studies on the impacts of historical mining contamination have focused on water quality and river ecology (Livingston, 1987; Pang, 1995; Webster, 1995; Harding et al., 2000; Harding and Boothroyd, 2004; Black et al., 2005; Harding, 2005; Webster-Brown and Craw, 2005; Boseley and Mauk, 2008). Studies of the legacy effects of the

96 historical discharge of mine tailings in New Zealand river sediments have
97 previously focused on either bedrock-confined channels (Shag River catchment in
98 Otago; Black et al., 2004), or small, short, steep catchments (catchments of the
99 western Coromandel Peninsula between Waiomu and Thames; Craw and
100 Chappell, 2000), which lack substantial floodplains. It has been found that in such
101 systems the historical mine waste has been effectively flushed from these
102 catchments. However, in the large floodplain system of the Ohinemuri and
103 Waihou rivers historical documentation shows that large amounts of mine waste
104 was deposited on the floodplain during flood events in the early twentieth
105 century (AJHR, 1910), and studies of water quality in the Waihou River show
106 ongoing contamination of water and suspended sediment (Webster, 1995). This
107 study aims to fill this knowledge gap by quantifying the contamination legacy of
108 mine waste discharged by historic gold mining activities preserved in the
109 floodplains of the Ohinemuri and Waihou rivers.

110

111 **2. Study area**

112 *2.1. Historical gold mining activities in the Coromandel region and their*
113 *environmental impacts*

114 Historical gold-mining activities in New Zealand were principally focused in the
115 South Island goldfields of Nelson and Marlborough, Westland, Otago, and
116 Southland, and the North Island goldfields located on the Coromandel Peninsula.
117 Alluvial gold was first discovered near Coromandel town in the north of the
118 peninsula in 1852, triggering a short-lived gold rush (Downey, 1935; Salmon,
119 1963; Moore and Richie, 1996). Subsequent discoveries of gold-bearing quartz
120 reefs to the south led to the establishment of the Coromandel goldfield in 1862

and the Thames goldfield in 1867 (Weston, 1927; Downey, 1935; Salmon, 1963). By the late 1860s there was considerable expectation among prospectors that the Ohinemuri River catchment would be opened up for mining (Moore and Richie, 1996). However, the Ohinemuri catchment was Maori land and the local chief was emphatically opposed to mining; six years elapsed before an agreement was reached (Salmon, 1963; Moore and Richie, 1996). The Ohinemuri Goldfield was opened in March 1875 with a literal rush of over 800 prospectors seeking claims (McCombie, 1897).

Initial disappointment at the lack of alluvial gold in the Ohinemuri was tempered by the discovery of gold-bearing quartz reefs in the Waitekauri Valley and at Owharoa (Salmon, 1963; Moore and Richie, 1996). Substantial gold-bearing reefs were subsequently discovered at Waihi in 1878 (the 'Martha Reef'), and on Karangahake Mountain in 1882 (Weston, 1927; Downey, 1935; Salmon, 1963). However, the low-grade concentrations of gold and the sulphide content of the reefs defied initial attempts to profitably recover gold from workings across the Ohinemuri. Traditional methods of wet crushing and mercury amalgamation (Downey, 1935) were only able to recover around 45-50% of the gold content (Moore and Richie, 1996; Boseley and Mauk, 2008). The advent of the cyanide process for gold extraction, first trialled internationally on a large-scale commercial basis by New Zealand Crown Mines at Karangahake in 1899, provided an efficient method of gold extraction, enabling approximately 90% of the gold content to be recovered (Moore and Richie, 1996).

The waste-rock by-product of ore crushing and amalgamation or cyanide processing was discharged directly into the Ohinemuri River and its tributaries from stamper batteries throughout the catchment between 1875 and the early

1950s (AJHR, 1910, 1921; Ohinemuri Gazette, 1910; Morgan, 1988; Watton, 1995, 2006). Under pressure from mining companies the Mines Department Gazetted the Ohinemuri River as a 'sludge channel' in 1895, allowing unfettered discharge of mercury- and cyanide-contaminated tailings directly into the river (AJHR 1910, 1921; Watton, 1995, 2006).

There are differing estimates of the volume of tailings discharged into the Ohinemuri River and its tributaries. Contemporary estimates of the tailings discharged varied from between ~1500 Mg d^{-1} (~560,000 Mg yr^{-1}; AJHR, 1910), to about ~2030 Mg d^{-1} (~741,000 Mg yr^{-1}; Ohinemuri Gazette, 1910). Evidence presented before the Waiho and Ohinemuri Rivers Commission suggested that in the period 1895-1910 over 4,065,000 Mg of tailings were discharged into the Ohinemuri River and its tributaries (AJHR, 1910). The 1921 Rivers Commission later put the total volume of tailings discharged into the Ohinemuri River at ~6,098,000 Mg (AJHR, 1921). Morgan (1988) estimated that during its years of operation the Victoria Battery at Waikino was discharging 800 Mg of cyanide-impregnated tailings every day (~292,000 Mg yr^{-1}). Watton (1995) estimated the total yearly tailings discharge from all sources into the Ohinemuri River to be around 250,000 Mg yr^{-1}.

The discharge of mining waste into the Ohinemuri River and its tributaries resulted in the rapid silting-up and narrowing of the channel, with around 2,200,000 Mg of sandy tailings deposits estimated to be present in the riverbed downstream of Mackaytown in 1910 (Fig. 1; AJHR, 1910). Constriction of the river channel resulted in severe floods regularly depositing mine tailings on farmland adjacent to the river (Ohinemuri Gazette, 8 August 1900; AJHR 1910). A major flood on 14 January 1907 resulted in the extensive deposition of mine tailings

171 across the Ohinemuri and Waihou floodplains near Paeroa, causing widespread,
172 significant damage to property, farmland, and stock (Figs. 2, 3, and 4; AJHR,
173 1910). This was followed by further floods in 1908, 1909, and 1910, that brought
174 further destruction to the infrastructure of Paeroa township and surrounding
175 farmland (AJHR, 1910; Watton, 1995). In March 1910 the government bowed to
176 public pressure to investigate the silting of the Ohinemuri River and the
177 consequent flooding hazard, and established a commission of inquiry (AJHR,
178 1910). The commission recommended that the 1895 proclamation of the
179 Ohinemuri River as a sludge channel be revoked, and that flood protection
180 measures be undertaken. This initiated an ongoing, 115-yr-long programme of
181 flood control measures, including dredging the river channel, cutting new
182 channels for the river, and construction of stop-banks to constrain floodwaters
183 (Fig. 4; AJHR, 1910; Watton 1995). Beyond flood control measures, no
184 remediation efforts have been undertaken to counter the potential
185 environmental impacts of the discharge of mine waste into the Ohinemuri River.

186

187 *2.2. Physical geography, geology, tectonic setting, and gold mineralisation of the*
188 *Ohinemuri catchment*

189 The Ohinemuri River rises in the eastern Coromandel-Kaimai Ranges, and flows
190 west for about 28 km to join the Waihou River near the township of Paeroa (Fig.
191 1). The Ohinemuri River initially flows through the Waihi Basin formed in a
192 volcano-tectonic depression filled with early-Pleistocene and Pliocene ignimbrites
193 and lake deposits (Braithwaite and Christie, 1996; Christie et al., 2001; Ling,
194 2003). The Ohinemuri River has several small tributaries, including the Waitekauri
195 River that joins the Ohinemuri at Waikino, and the Waitawheta River that joins

196 the Ohinemuri at Karangahake (Fig. 1). At Karangahake the Ohinemuri River
197 changes character, becoming deeply entrenched within an antecedent, vertically-
198 sided gorge cut during the uplift and eastward tilting of the western Coromandel-
199 Kaimai Ranges (Henderson and Bartrum, 1913; Braithwaite and Christie, 1996).
200 West of the Karangahake Gorge, the Ohinemuri River exits the ranges and
201 meanders across the open country of the Waiho River floodplain. At Paeroa the
202 confluence of the Ohinemuri and Waihou rivers has been altered as part of the
203 Waihou flood protection scheme, with a cut made to shorten and straighten the
204 path of the Waihou channel and shift the Waihou-Ohinemuri confluence
205 downstream of Paeroa (Fig. 4).

206 The Ohinemuri River catchment covers approximately 287 km^2, the majority of
207 which is the hilly to mountainous terrain of the Coromandal-Kaimai Ranges (Fig.
208 1; Watton, 1995). Elevations within the catchment range from approximately 160
209 m to over 760 m. The steeper parts of the catchment are forest-covered, while
210 the lower-elevation eastern part of the catchment within the Waihi Basin is
211 rolling farm country (Watton, 1995). The climate of the catchment is warm and
212 wet: average temperatures for the catchment range from 18°C in the summer
213 months to 10°C in winter. The average annual rainfall in the high-relief north of
214 the catchment is 2700 mm yr^{-1}, falling to 1500 mm yr^{-1} in the south and in the
215 east towards the coast (Maunder, 1974; NIWA 2002). The Ohinemuri River has a
216 mean flow of 12 m^3/s and a minimum flow of 1.1 m^3/s, gauged at Karangahake
217 Gorge (cf. Fig. 1C). Monthly mean flow peaks at ~20 m^3/s in June, with a minimum
218 monthly mean flow of ~6 m^3/s in January. Given the compact nature of the
219 catchment, high relief, high rainfalls, and lower than average permeability, the
220 Ohinemuri River has a time of concentration of around six hours (Watton, 1995).
221 The largest flood in the Ohinemuri since records began in 1956 occurred on 13

April 1981 during the Waikato Storm, with a peak discharge of 1047 m^3/s recorded at Karangahake (NIWA, 2002). The largest historic flood in the catchment was the 1910 flood (Jane and Green, 1983), during which the Ohinemuri River reached a peak stage of 42.18 m (compared to only 18.66 m in 1981; NIWA Historic Weather Events Catalog). Historically, flood events typically occur in late summer, associated with ex-tropical cyclones (De Lisle, 1967; Jane and Green, 1983; Phillips, 2000).

The gold deposits of the Ohinemuri Goldfield occur as quartz veins produced by epithermal mineralisation driven by hydrothermal systems associated with late Miocene subaerial volcanism (Brathwaite and Christie, 1996; Christie et al., 2007, 2008; Mauk et al., 2011). Mineralisation is tectonically-controlled, with the quartz veins occupying high-angle extensional fractures opened predominantly by normal dip-slip movement (Christie et al., 2008; Mauk et al., 2011). Individual deposits occur as vein systems formed of arrays of extensional veins surrounded by zones of hydrothermally-altered rock that range in size from ~5-14 km.

3. Methods and materials

Bulk samples of approximately 150 g were taken from overbank (Wi-1) and channel sediments (Ke-1 to Ke-4) along the course of the Ohinemuri River (Fig. 4). Bulk samples were also taken from floodplain profiles in exposed riverbanks (Oh-1 to Oh-5, and Wai-1 to Wai-4), and percussion cores (G and M) were collected within the study reach (Fig. 4). Floodplain profiles were sampled to track downstream and lateral variations in grain size and geochemistry. Floodplain cores characterise flood-basin deposits to provide a long-term Holocene

246 sedimentation context, whereas the near-channel floodplain profiles capture
247 historic and mining-age sedimentation.

248 Floodplain core M was split, with one half sampled and analysed for As, Cu, Fe,
249 Pb, and Zn using hand-held XRF (Table 1; Niton XLt 700 series, Thermo Fisher
250 Scientific, Germany, internal calibration of the instrument recalibrated annually).
251 Floodplain core G was also analysed using hand-held XRF Niton to measure As,
252 Cu, Fe, Pb, and Zn (Table 1).

253 Riverbank and in-channel bulk samples (Wi-1, Ke-1 to Ke-4, collected in February
254 2014) were air dried and sieved, and the <0.63 µm fraction was used for
255 geochemical analysis. A subsample of 0.5 g was treated with 2 ml of nitric acid
256 and left for 1 hr, after which 18 ml of distilled water was added. Following HF-
257 HNO_3 digestion, concentrations of As, Ag, Hg, Pb were determined using
258 inductively coupled plasma mass spectrometry (Table 1; ICP-MS, Thermo-
259 Finnegan Element 2 Magnetic Sector ICP-MS, Thermo Scientific, Germany), and
260 Cu and Zn were analysed using atomic absorption spectrometry (Table 1; AAS,
261 Perkin Elmer AAnalyst 400, USA). A comparison was made of the Niton XRF
262 measurements of Pb and As with ICP-MS measurements of the same elements, as
263 well as a comparison of the Cu and Zn concentrations measured by both the
264 Niton XRF and AAS (Supplemental Table 1), with measured concentrations from
265 all three instruments showing suitable correlation.

266 Concentrations of As, Cu, Fe, Pb, Zn in sediments from riverbank sections (Oh-1 to
267 Oh-5, Wai-1 to Wai-4, collected in February 2015) were analysed, following air-
268 drying, sieving, extraction of the <0.63 µm fraction, and digestion in HF-HNO_3,
269 using inductively coupled optical emission spectrometry (Table 1; ICP-OES, Varian
270 720-ES, axial configuration, using a simultaneous solid state detector, CCD). The

precision and accuracy of the digestions was determined using duplication samples to 10% of the total number of samples, and with certified soil reference material GBW07404 for ICP-OES measurements and standard reference material NIST 1643a for ICP-MS measurements. Average precisions ranged between 3-8%, and average accuracies between 5-11%. Correlation of the 2014 and 2015 datasets was achieved by comparing the results for the mine waste layer in Oh-3, which was analysed in both years. The 2015 results for As, Cu, Fe, Pb and Zn are within 10% of the 2014 results.

Sediment samples of approximately 4 g were taken at 10 cm intervals along the length of cores M and G for particle size analysis. Approximately 30 ml of hydrogen peroxide (25%) was added to each sediment sample and left to react. Once the chemical reaction ceased samples were centrifuged at 5000 rpm for 5 min. Each sample was then decanted, washed with distilled water, and centrifuged again, with the process repeated until all the hydrogen peroxide was removed. Each sample was agitated before analysis to prevent flocculation. Particle size was analysed using a Horiba Partica LA-950v2 laser scattering particle size distribution analyser, with each sample analysed three times.

Fragments of wood and charcoal recovered from the percussion cores M and G were radiocarbon-dated at the University of Waikato Radiocarbon Dating Laboratory using accelerated mass spectrometry (AMS) dating (Table 2). Conventional radiocarbon ages were calibrated to sidereal years using Calib 7.1 (Stuvier and Braziunas, 1993; Stuvier and Reimer, 1993), and the Southern Hemisphere calibration curve SHCal04 (McCormac et al., 2004). All calibrated radiocarbon ages are presented using the 2-sigma uncertainty term (95% degree of confidence).

296

297 **4. Results**

298 *4.1. Pre-mining floodplain stratigraphy*

299 The Ohinemuri floodplain sediments in cores M and G largely comprise fine-
300 grained clayey silts (Figs. 5 and 6). A tephra unit is preserved in core G at 120-130
301 cm, which is constrained by a ^{14}C age from a sample of fossilised wood at 100 cm
302 depth of 8790 ± 190 cal BP (Fig. 5). According to Lowe et al. (2013), this tephra
303 layer could be deposited either in conjunction with the Rotoma event (c. 9472 ±
304 40 cal BP) or the Opepe event (c. 9906 ± 246 cal BP). A tephra unit is also present
305 in the floodplain profile Oh-3 at a depth of 150 cm (Fig. 7), though no organic
306 material was present to constrain the age of this tephra. Fine-grained
307 sedimentation characterised the Ohinemuri floodplain during the Holocene
308 through to European settlement, with a mid-Holocene ^{14}C age from fossil rootlet
309 material at 160 cm in core M of 5870 ± 120 cal BP (Fig. 6).

310

311 *4.2. Post-mining floodplain stratigraphy*

312 Mapping of the 1907 mine waste flood deposit, described as a dirty yellow-brown
313 talcum-like silt (AJHR, 1910, Phillips, 1986; Watton, 2006), indicates dispersal
314 across the area where core G was recovered (Fig. 4). This layer has previously
315 been described by Philips (1986) from archaeological excavations of Raupa Pa and
316 Waiwahu Pa, between 0.5-1 km from the locations where cores G and M were
317 recovered. However, core G contains no yellow silt unit, and concentrations of
318 elements characteristic of mine tailings such as Pb, As, and Cu, are low (Fig. 5).
319 Core M contains an 18 cm thick unit of yellow-coloured silty sand between 42-60

cm depth. This unit contains high concentrations of Pb, As, and Cu (Fig. 6). Above the yellow silty sand unit floodplain sediments in core M consist of silty sands, of a much coarser grade than pre-European sediments.

A downstream sequence of historic floodplain sedimentation is given in sites Oh-1 to Oh-5 and Wai-4 to Wai-1 (Figs. 8 and 9). Sites Oh-1 and Oh-2, together with percussion cores M and G, are located upstream of the pre-1910 confluence of the Ohinemuri and Waihou rivers (Fig. 4). The most upstream site (Oh-1), within the Karangahake Gorge, contains several yellow-coloured silty sand units, each containing high concentrations of Pb, As, and Fe (Figs. 7 and 8). Oh-2 contains a similar yellow-coloured silty sand unit, also with high concentrations of Pb, As, and Fe (Fig. 8).

The floodplain profile exposed in the cut bank of the Ohinemuri River at site Oh-3 features a 20 cm thick yellow silty sand unit with high concentrations of Pb, As, and Fe (Fig 7). This is overlain by a 100 cm thick sequence of fluvial silts and sands. At Oh-4, there is a 20 cm thick yellow silty sand unit with high Pb, As, and Fe concentrations, overlain by 100 cm of brown fluvial sands (Figs. 7 and 8). Oh-5 similarly features a 70 cm thick yellow silty sand unit with a similar geochemical signature, overlain by an 80 cm thick unit of light brown sand. Sites Oh-4 and Oh-5 are both distinguished by coarser, sandy sediments (Fig. 7).

Downstream of the pre-1910 confluence, sections Oh-3 to Oh-5 and Wai-4 to Wai-1 are located along the pre-1910 Waihou River course (Fig. 4). Sections Wai-1 to Wai-3 do not feature the yellow silty sand unit found in core M and sections Oh-1 and Oh-2, and comprise sequences of silty sands and coarse sand (Fig. 9). At Wai-4, the most downstream section, a 15 cm thick layer of finely-layered, pale grey and orange, silty sands featuring high concentrations of Pb, As, Zn, and Cu is

preserved at 45-60 cm depth (Fig. 9). This unit is overlain by 45 cm of clayey silt.

4.3. *Floodplain geochemistry*

As described above, a yellow silty sand unit is commonly identified in river bank sections along the course of the Ohinemuri and Waihou rivers downstream of the Karangahake Gorge. This unit matches historical descriptions of the mine tailings deposited on the Ohinemuri floodplain during the 1907 flood (AJHR, 1910). The yellow silty sand unit preserved in core M and sections Oh-1 to Oh-5 and Wai-4 is characterised by high concentrations of Pb, Cu, and As.

As previously noted, percussion core G does not feature a yellow silty sand layer (Fig. 5). Concentrations of contaminant metals and As are low throughout the length of the core, except in the tephra layer which has elevated concentrations of Pb (~40 mg kg^{-1}), Zn (~200 mg kg^{-1}), As (~20 mg kg^{-1}), and Fe (~40,000 mg kg^{-1}). As this core covers the period from the early Holocene back to c. 8800 cal BP, it provides a useful context for characterising the pre- and post-mining sediment geochemistry in the Ohinemuri catchment.

In core M, below 150 cm depth, early Holocene background concentrations of contaminant metals and As are low: Pb <30 mg kg^{-1}; Fe <30,000 mg kg^{-1}; As <17 mg kg^{-1}; and Cu <50 mg kg^{-1} (Fig. 6). A minor increase in Pb, Zn, and As concentrations compared to background levels at 211-215 cm depth coincides with an influx of sand. The Zn concentration in the core increases from 160 mg kg^{-1} at 190 cm depth, to 370 mg kg^{-1} at 125 cm; this peak coincides with a clayey silt unit from 104-150 cm depth. Concentrations of Pb, Cu, and As peak between 42-60 cm depth in a yellow silty sand unit. Above this yellow silty sand unit

concentrations of Pb, Cu, and As are significantly elevated compared to the low background concentrations exhibited in the lower part of the core (Fig. 6).

The floodplain profile Oh-1 exhibits peak concentrations of Pb (570 mg kg^{-1}) and As (73 mg kg^{-1}) between 250-260 cm depth, coincident with a yellow silty sand unit (Fig. 7). Three thin (3-4 cm thick) yellow silty sand units are evident lower in the profile, and exhibit concentrations of Pb and As, that while lower, are significantly elevated when compared to the early Holocene background concentrations present in cores G and M (Figs. 6 and 7). Background concentrations of Zn and Cu do not vary significantly throughout the profile.

Downstream of Oh-1, floodplain profiles Oh-2, Oh-3, and Oh-4 all exhibit similar peak concentrations of Pb (320-540 mg kg^{-1}) and As (55-69 mg kg -1) in single, thick (10-50 cm) yellow silty sand units (Fig. 7). In the sediment above and below the yellow silty sand unit, concentrations of Pb and As are much lower, in line with background concentrations exhibited in cores M and G (Figs. 5 and 6). In section Oh-5, Pb and As concentrations are elevated in a yellow silty sand unit. However, peak concentrations of Pb and As, as well as peaks in Zn and Cu concentrations are observed immediately below this unit, between 135-150 cm depth, in a grey silty sand unit (Figs. 7 and 10). This is either a primary signature representing deposition of mine waste from a flood event prior to 1907, or it may reflect chemical remobilisation of the As, Cu, Pb and Zn. The grey colour (Fig. 10) may be due to reductive dissolution of As-, Cu-, Pb- and Zn- Fe-bearing minerals in the sands (cf., McArthur et al., 2004; Kossoff et al., 2011) and downward remobilisation of the metalloid and metallic elements (cf., Hudson-Edwards, et al., 1998). The remobilised elements may have then been redeposited in secondary Fe hydroxides like those in Fig. 10.

In floodplain profiles Wai-1 to Wai-3 (Fig. 9), concentrations of As, Cu, and Fe are close to early Holocene background levels exhibited in cores M and G. Concentrations of Pb and Zn in these floodplain sections are slightly elevated (Pb 100-300 mg kg^{-1}; Zn ~100 mg kg^{-1}) compared to background levels, though concentrations of both metals are well below levels exhibited in yellow silty sand mine-waste flood deposits found in other locations. Floodplain profile Wai-4, well downstream of the mapped extent of the 1907 floodplain deposit, exhibits a yellow silty sand unit with high concentrations of Pb and As, and peak concentrations of Zn and Cu at the base of the unit (Fig. 9).

4.4. Overbank and channel deposit bulk sediment geochemistry

Bulk sediment samples of in-channel sediments (Ke-1 to Ke-4) and overbank alluvial deposits (Wi-1) were recovered from the Ohinemuri River within the Karangahake Gorge, from the Ohinemuri River immediately downstream of Waihi town, and from the Waitekauri River, a major tributary of the Ohinemuri (Fig. 4). Samples Wi-1 and Ke-3 (Table 3) showed elevated concentrations of Pb (104-110 mg kg^{-1}), Zn (140-320 mg kg^{-1}), and Ag (2.5-2.9 mg kg^{-1}) compared to the Holocene background levels measured in cores M and G. However, these concentrations are much lower than those measured in the yellow sandy silt unit found across the Ohinemuri floodplain. In samples Ke-1, Ke-2 and Ke-4 (Table 3) concentrations of Pb, Zn, Cu, and Ag were in line with background levels. The concentration of As in sample Ke-2 (40 mg kg^{-1}) is in line with As concentrations measured in the yellow silty sand unit found in core M (Fig. 6) and sections Oh-1 to Oh-5 (Fig. 7). All samples showed elevated concentrations of Hg (0.3-0.5 mg kg^{-1}).

5. Discussion

5.1. The 1907 flood mine-waste deposit

Historic mapping of the 1907 mine-waste flood deposit, described as a dirty yellow-brown talcum-like silt (AJHR, 1910, Phillips, 1986; Watton, 2006), indicates widespread dispersal across the Ohinemuri floodplain. A yellow silty sand unit characterised by high concentrations of Pb, As, and Fe, interpreted to be the 1907 mine waste flood deposit, can be traced for ~20 km along Ohinemuri and Waihou river courses downstream from the Karangahake Gorge. The distribution of this deposit in the cores and floodplain sections is more extensive than was historically mapped (cf. Fig. 5). The thickness of the mine-waste flood deposits and post-mining alluvium progressively thins with increasing distance downstream from the Karangahake Gorge, from more than c. 300 cm at Oh-1 to ~15 cm at Wai-4.

In core M, the yellow silty sand unit with high concentrations of Pb, As, and Cu (Fig. 6) is interpreted, based on the visual, sedimentological, and geochemical characteristics, as mine-waste tailings deposited on the floodplain in the 1907 flood. Core G contains no yellow silt unit (Fig. 5), despite the core being recovered from an area indicated to have been inundated by mine waste similar to core M (see Fig. 4). The absence of mine waste in core G is interpreted as post-1907 agricultural development ('humping and hollowing' – a practice of mechanically contouring the land into long, low ridges ['humps'] interspersed with shallow drainage ditches ['hollows'] to improve drainage and pasture production; e.g., McDowell, 2008; Horrocks et al., 2010) in that location removing the upper layer of floodplain sediments containing the 1907 mine-waste flood deposit.

Section Oh-1 is located on a fluvial bench inset beneath the spatially-restricted fluvial terrace on the true-left of the Karangahake Gorge (Figs. 4 and 11). Oh-1 features four yellow silty sand units with elevated concentrations of Pb and As interbedded with course sand units (Fig. 7). The uppermost, thicker (~20 cm thick) yellow silty sand unit with peak Pb and As concentrations is interpreted as the 1907 mine-waste flood deposit. This extends the historic mapping of the 1907 flood deposit, which did not record mine-waste flood deposits within the Karangahake Gorge (Fig. 4). The three thinner (~3-4 cm thick) yellow silty sand units below are interpreted as deposits from smaller, pre-1907 floods. These smaller flood events are likely to have been of sufficient magnitude to deposit mine waste on the inset bench within the confinement of the gorge, but were insufficient to overtop the Ohinemuri's banks downstream of the gorge. Therefore it is possible that the only record of these lower-magnitude flood events lies within the spatial confinement of the gorge (cf. Fig. 12).

Downstream of Oh-1, floodplain profiles Oh-2, Oh-3, and Oh-4 all contain a similar yellow silty sand unit with peak concentrations of Pb and As that is interpreted to be the 1907 flood mine-waste deposit (Fig. 7). In section Oh-5, Pb and As concentrations are elevated in a yellow silty sand unit interpreted to be the 1907 flood mine-waste deposit. However, peak concentrations of Pb and As, as well as peaks in Zn and Cu concentrations, are observed immediately below this unit between 135-150 cm depth in a grey silty sand. This lower unit is interpreted to be reduced mine waste (Fig. 10).

Mine waste is absent from floodplain profiles Wai-1 to Wai-3 (Fig. 9), though all three locations are sited within the historically-mapped extent of the 1907 flood mine-waste deposits (Fig. 4). The historic mapping of the 1907 flood deposits

468 describes the mine waste to the north of Wai-2 as a “light silt deposit”. It is
469 therefore possible that visual evidence of the deposits at Wai-1 to Wai-3 was
470 obscured by post-flood bioturbation or agricultural practices. Mine waste at Wai-
471 2 may have been removed during the emplacement of the Waihou cut, designed
472 to shift the Waihou-Ohinemuri confluence to the west and straighten the Waihou
473 channel (Fig. 4). A thin layer (~15 cm) of yellow silty sand with elevated
474 concentrations of Pb and As, interpreted to be the deposit of the 1907 flood, is
475 present at Wai-4 (Fig. 9), approximately 2.5 km downstream of the historically-
476 mapped extent of the 1907 flood deposit (Fig. 4). As with Oh-5, peak
477 concentrations of Pb, As, as well as peaks in Zn and Cu are observed immediately
478 below the mine-waste unit, and this is interpreted as post-deposition reduction of
479 the mine-waste deposit.

480

481 *5.2. Volume of the 1907 mine-waste flood deposit stored in the floodplain*

482 The mapped extent of the 1907 mine-waste flood deposit (AJHR, 1910), coupled
483 with our new data on the thickness of the deposits at the channel edge, provides
484 a basic framework from which to estimate the volume of mine waste currently
485 stored in the Ohinemuri and Waihou river floodplains (Table 4). The historically-
486 mapped extent of the mine waste deposit (AJHR, 1910) was extended
487 downstream to include Wai-4, where mine waste was located in the floodplain
488 section, but was not historically mapped (Supplemental Fig. 1). The mapped
489 extent of the mine-waste deposit was also expanded in the vicinity of
490 Mackaytown, to include inset terraces downstream of Oh-1, where mine waste
491 was also located in this study but not historically mapped. The thickness of the
492 mine waste at the channel edge of each polygon in the mapped extent

493 (numbered 1 to 18 on Supplemental Fig. 1) was taken from cores and floodplain
494 sections examined in this study (Table 4; cf. Figs. 6, 7 and 9). In order to account
495 for the decreasing thickness of mine waste with increasing distance from the
496 channel, a factor of 0.65 was applied to the volume of mine waste calculated for
497 each polygon. This factor follows the simple case where the mine waste thickness
498 decreases from 100% at the channel edge, to 30% at the distal margin of the
499 mapped extent. This assessment suggests the volume of solid mine waste
500 deposited on the floodplain by the 1907 flood event to be approximately
501 1,130,000 m^3 (Table 4). Assuming an average density of 2 Mg/m^3 this equates to
502 2,260,000 Mg of mine waste, approximately 38% of the amount estimated to
503 have been discharged into the Ohinemuri River between 1895-1910 (AJHR, 1921).
504 This estimate does not include mine waste within the channel, which was
505 estimated to be approximately 2,200,000 Mg in the riverbed downstream of
506 Mackaytown in 1910 (AJHR, 1910). These volumes of mine waste are extremely
507 large in a New Zealand context (cf. Black et al., 2004).

508 In comparison with the 2014 Mount Polley (25 M m^3, Bryne et al., 2017) and 1998
509 Aznalcóllar (7 M m^3, Hudson-Edwards et al., 2003) tailings dam failures, the
510 dispersal and deposition of ~1.13 M m^3 in the 1907 flood would appear to have
511 been globally a relatively small spill. However, it was significantly larger (c. 10
512 times) than the well-publicised 1996 South American Porco (0.235 M m^3, Macklin
513 et al., 2006) as well as the 2000 Romanian Baia Mare (0.1 M m^3, Macklin et al.,
514 2006) and Baia Borsa (0.12 M m^3, Macklin et al., 2006) accidents. This indicates
515 that it constituted, and was recognized at the time, a significant
516 geomorphological and environmental event. Indeed, it prompted the creation
517 and subsequent investigations of the Waihou and Ohinemuri Rivers Commission,

518 a nationally significant event in the history of environmental regulation in New
519 Zealand.

520 Estimates of the mine waste stored in other historical mining-affected
521 catchments are normally given as area rather than volume measurements since
522 thicknesses cannot be determined unless coring is carried out, as we have done
523 for this study. For example, the extent of metal contamination in floodplains of
524 the mining-affected Río Pilcomayo in Bolivia, River Swale in northern England and
525 Belle Fource River in the USA have been reported as 35 km^2, 25.4 km^2 and 14.5
526 km^2, respectively (Andrews, 1987; Dennis et al., 2008; Balaban et al., 2015). If
527 average thicknesses of these deposits are assumed to be 1 or 2 m, then these
528 areas translate as volumes of 35 or 70 M m^3, 25.4 or 50.8 M m^3 and 14.5 or 29 M
529 m^3, respectively. These are all significantly larger than the 1.13 M m^3 of mining-
530 affected material estimated to be contained in the Ohinemuri system, re-
531 emphasising the relative small size of this system on a global scale.

532 *5.3. Floodplain sedimentation rates*

533 The 1907 flood mine-waste deposit provides a distinctive stratigraphic horizon
534 that may be used to evaluate pre- and post-mining sedimentation rates in the
535 Ohinemuri catchment. The radiocarbon date from core G indicates a pre-
536 European floodplain sedimentation rate of ~0.09 mm yr^{-1}, though this is
537 interpreted to be a minimum rate as agricultural practices may have removed
538 floodplain sediment from this location (Fig. 5). In core M the radiocarbon age and
539 mine-waste layer suggest that prior to the onset of European mining activities,
540 the long-term average Holocene sedimentation rate was ~0.2 mm yr^{-1} over the
541 past c. 8800 cal BP.

Post-mining sedimentation rates may be reconstructed using the mine-waste layers found across the floodplain. In core M, the rate of floodplain sedimentation accelerated by an order of magnitude to ~5.5 mm yr^{-1} in the upper 60 cm of the core that is delimited by the 1907 mine-waste flood deposit (Fig. 6). In the floodplain profiles, the highest rate of post-mining sedimentation is recorded at Oh-2, at ~26.8 mm yr^{-1}. The post-mining sedimentation rate is similar at Oh-1, at ~22.5-24.5 mm yr^{-1}. Post-mining sedimentation rates decrease downstream to ~10 mm yr^{-1} between Oh-3 to Oh-5, and fall to the lowest rate of ~5.5 mm yr^{-1} at Wai-4 (Fig. 12). These rates correspond with the broadening of the floodplain, (Fig. 11). In all sections the anthropogenic sedimentation rate is an order of magnitude greater than background Holocene sedimentation rate recorded in cores G and M.

While it has been noted anecdotally that historic gold mining activities in Golden Bay, Otago, and Coromandel resulted in significant increases in sediment supply in mining-impacted catchments (Black et al., 2004; Fuller et al., 2015), there have been no quantitative measures of the change in sedimentation rates in response to mining activities in New Zealand. In Northland the impact of Maori and European settlement on sedimentation rates has been explored by Richardson et al. (2013, 2014). Background Holocene sedimentation rates in Northland were ~<1 mm yr^{-1}. In the past ~500 yr, Richardson et al. (2013, 2014) observed acceleration in floodplain sedimentation rates to ~8-13.5 mm yr^{-1} in the Northland Region. Follow-up work at Kaeo in Northland suggests sedimentation rates increased to at least 25 mm yr^{-1} in the last 50 yr (Fuller et al., 2015). These accelerated rates of sedimentation have been attributed to post-settlement deforestation, initiated by Polynesian settlement, and exacerbated by European colonisation, which mirrors a similar pattern of late-Holocene acceleration in

568 sedimentation rates observed elsewhere in the world (Macklin et al., 2010;
569 Turner et al., 2010; Macklin et al., 2014).

570 Holocene pre-Polynesian settlement sedimentation rates for the Ohinemuri
571 catchment (cores M and G) are similar to those observed in Northland by
572 Richardson et al. (2013, 2014). Peak post-mining sedimentation rates in the
573 Ohinemuri (Oh-1 and Oh-2) are around double the post-settlement (Polynesian)
574 sedimentation rates observed in Northland, although they are equivalent to those
575 observed in the last ~50 yr at Kaeo (Fuller et al., 2015). At sites downstream of
576 the Karangahake Gorge on the Ohinemuri floodplain (Oh-3 to Oh-5, and Wai-4),
577 post-mining sedimentation rates (~5.5-10 mm yr^{-1}) are similar to more region-
578 wide post-settlement sedimentation rates in Northland catchments (8-13.5 mm
579 yr^{-1}). However, the Ohinemuri rates downstream of the Karangahake Gorge occur
580 in an unconstrained floodplain setting (Fig. 11), while the Northland rates come
581 from catchments with confined accommodation space (Richardson et al., 2014).
582 Given the geomorphic context, the post-mining sedimentation rates observed in
583 the Ohinemuri catchment are therefore significant, and speak to the volumes of
584 mine waste being discharged into the system during the period between 1875-
585 1955.

586

587 *5.4. Downstream contamination trends and influence of fluvial geomorphology*
588 *on contaminant storage*

589 Downstream trends in the concentration of Pb, As, and Cu, the thickness of the
590 1907 flood deposit, the mean grain size of the 1907 flood deposit, and the 1907-
591 present sedimentation rate are shown in Fig. 12. The concentrations of Pb, As,
592 and Cu in the mine-waste flood deposit do not change systematically down the

593 length of the Ohinemuri Valley (Fig. 12A). This contrasts with other studies of
594 mining contamination in floodplains that have observed a downstream decrease
595 in metal and metalloid concentrations (e.g., Leigh, 1997; Hudson-Edwards et al.,
596 2001; Dennis et al., 2003; Miller and Orbock Miller, 2007; Lecce and Pavlowsky,
597 2014). These examples document the gradual downstream dispersal of mine
598 waste over periods of c. 200-500 yr. In the case of the Ohinemuri catchment, the
599 dispersal of mine waste across the floodplain occurred in a single extreme event,
600 akin to the failure of a tailings dam (cf. Graf, 1990; Hudson-Edwards et al., 2003).
601 The flood had sufficient capacity to easily convey the mine waste down the length
602 of the valley, and as a result there is no systematic downstream decrease in
603 geochemical concentrations in the Ohinemuri. This echoes the findings of Graf
604 (1990), who also observed incongruence with hydraulic and geomorphic theory in
605 thorium-203 concentrations that fluctuated irregularly with distance downstream
606 from a tailings-dam failure.

607 Distance downstream is also a poor predictor of the thickness of the mine-waste
608 flood deposit (Fig. 12B). The thickest mine-waste deposits occur at sites Oh-2 and
609 Oh-5, which appear as outliers compared with the population of other sites.
610 While previous research has indicated that catchment-scale geomorphic factors
611 influence contaminant storage trends (e.g., Graf, 1983; Magilligan, 1985, 1992;
612 Lecce, 1997; Lecce and Pavlowsky, 2014), the degree of variance in the
613 downstream thickness of the mine-waste deposit in the Ohinemuri suggests that
614 local geomorphic factors are significant. In the case of Oh-2, this site is
615 approximately 1.2 km downstream of where the Ohinemuri River exits the
616 Karangahake Gorge, and is immediately upstream of the confluence with Tarariki
617 Stream which flows into the Ohinemuri on the true-right (Fig. 11). The
618 pronounced deposition of mine waste in this location (Fig. 12B) is interpreted to

reflect both the proximity of the site to the source of mine waste in the gorge, and a drop in stream power as the floodwaters overtopped the channel banks upon exiting the gorge. Flood waters in the main Ohinemuri channel may have also been impeded by the discharge of water from the Tarariki Stream, resulting in enhanced deposition of mine waste at Oh-2. Cross section 2 (Fig. 11) indicates that this part of the river system has been the locus of deposition, since the Ohinemuri floodplain is perched some 5 m above the Waihou floodplain to the east. Accelerated deposition and enhanced thickness of mining wastes in this vicinity is therefore to be expected in this geomorphic context. Further downstream at Oh-5, the Ohinemuri River is forced to make an abrupt left turn by low hills formed from weathered volcanic rocks (Fig. 11). The significant thickness of mine waste at Oh-5 is interpreted to reflect the 'ponding effect' of these low hills, which form a shallow basin on the true-right of the Ohinemuri channel where Oh-5 is situated (Figs. 4 and 11). The lower thickness of mine waste observed at the other sample locations on the Ohinemuri floodplain, between core M and site Wai-4, reflects diffuse overbank sedimentation on the low gradient floodplain at a significant distance from the source area of the mine waste (cf. Leigh, 1997; cf. Fig. 11).

Both the mean grain size of the 1907 mine-waste flood deposit and the post-1907 sedimentation rate display significant downstream trends (Figs. 12C and 12D). Mean grain size decreases with increasing distance downstream, reflecting a reduction in stream power in the lower reaches of the Ohinemuri as the channel gradient reduces. The lack of correlation between downstream distance and geochemical concentration (Fig. 12A) suggests that Pb, As, and Cu concentrations are independent of the mine waste grain size. The strong correlation between downstream distance and post-1907 sedimentation rate reflects the widening of

645 the floodplain downstream of the Karangahake Gorge and the dispersal of
646 sediments across a broader area.

647 The downstream trend in storage of the 1907 mine waste deposit is quite striking
648 (Table 4; Supplemental Fig. 1). The volume of mine waste calculated to be stored
649 within the Karangahake Gorge accounts for only 1.5% of the total volume. This
650 reflects both the limited accommodation space for deposition and higher stream
651 power within the gorge (Fig. 11; cf. Graf, 1983; Magilligan, 1985, 1992; Lecce,
652 1997; Lecce and Pavlowsky, 2014). The 'heavy silt deposits' mapped immediately
653 downstream of the gorge (AJHR, 1910) account for a significant 37.5% of the total
654 volume of stored mine waste in the Ohinemuri floodplain. As discussed above,
655 this reflects both proximity to the source of the waste, and a significant drop in
656 stream power as the floodwater exited the gorge (Fig. 11). Mine waste deposits
657 downstream of the 1907 confluence between the Ohinemuri and Waihou rivers
658 (between core G and site Oh-3) account for only 25.5% of the volume of waste
659 stored in the floodplain; 74.5% of the total volume of mine waste is thus stored in
660 the floodplain upstream of the Ohinemuri-Waihou confluence. This distribution of
661 storage is similar to the situation described by Lecce and Pavlowsky (2014) in the
662 Dutch Buffalo Creek watershed, where the majority of historic mine waste is
663 stored in the upper reaches of the mined tributary. Downstream of the
664 Ohinemuri-Waihou confluence, there is both a dilution and a dispersal effect as
665 the Ohinemuri joins the larger Waihou (cf. Fig. 1). That such a clear mine waste
666 deposit should be detected in the Waihou floodplain at Wai-4 demonstrates the
667 significance of the 1907 event in dispersing this contaminated material and
668 speaks to the volume of this sediment in the context of this catchment.

669

5.5. Environmental legacy and significance of historical gold mining activities in the Ohinemuri catchment

The Australian and New Zealand Guidelines for Fresh and Marine Water Quality (ANZECC and ARMCANZ, 2000) outline interim sediment quality guidelines (ISQG) for aquatic ecosystems. The guidelines provide two values for metal contaminants: concentrations below the ISQG-low threshold are unlikely to be toxic; while those exceeding the ISQG-high threshold are likely to be toxic (Table 5). Concentrations within the range between the ISQG-low and ISQG-high values are likely to pose a moderate risk to aquatic organisms.

The layer of mine-waste sediment in core M exceeds the ISQG-high thresholds for Pb and As, and exceeds the ISQG-low threshold for Cu (Fig. 6). Peak concentrations of Zn, while not coincident with the mine-waste layer, exceed the ISQG-low threshold, and come close to the ISQG-high threshold.

In the floodplain profiles Oh-1 to Oh-5 and Wai-1 to Wai-4, 100% of the samples exceed the ISQG-low threshold for Pb, while 41% of the samples also exceed the ISQG-high threshold (Figs. 7 and 9). Concentrations of As exceed the ISQG-low threshold in 44% of the samples, and exceed the ISQG-high threshold in 6% of the samples. Concentrations of Zn are below the ISQG-low threshold in all but two samples (91%), both of which exceed the ISQG-high threshold for Zn. Concentrations of Cu are below the ISQG-low threshold in 88% of the samples; 12% of the samples exceed the ISQG-low threshold.

The bulk sediment samples recovered from in-channel (Ke-1 to Ke-4) and overbank locations (Wi-1) within the Ohinemuri catchment generally contain low levels of contaminant metals at concentrations below the ISQG-low thresholds; no samples contained metal or metalloid concentrations that exceeded the ISQG-

high threshold (Table 3). Concentrations of As exceeded the ISQG-low threshold in 80% of the samples, while Pb and Ag concentrations exceeded the ISQG-low threshold in 40% of the samples. Only one sample exceeded the ISQG-low threshold for Zn, while all bulk sediment samples exceeded the ISQG-low threshold for Hg (Tables 3 and 5).

Metal and metalloid contaminants in river sediments in the Ohinemuri and Waihou catchments have previously been analysed by Beaumont et al. (1987), Webster (1995), and Sabti et al. (2000). The concentrations of contaminant metals in the in-channel and overbank bulk sediment samples recovered for this study are consistent with the findings of these earlier studies. The concentrations of contaminant metals are spatially variable, and likely reflect local factors such as the extent of disturbance, style and scale of mining and ore processing activities, flow rates, and the grain size of tailings (cf. Beaumont et al., 1987).

Contaminant metal and metalloid concentrations in the mine-waste layer located throughout the Ohinemuri pose a moderate to high risk to the Ohinemuri ecosystem. Pb and As occur in potentially toxic concentrations throughout the catchment, while Zn is found in potentially toxic concentrations in distinct locations, possibly as a result of chemical remobilization. Cu concentrations are unlikely to be toxic, though at those sites where the mine waste contaminants have been remobilized, Cu poses a moderate risk to the aquatic ecosystem. However, the averages and ranges of Ohinemuri As, Cu, Pb and Zn concentrations are generally lower than those in other alluvial river systems elsewhere in the world affected by mining activity (Table 6).

5.6. Risks of remobilisation of mine waste in the Ohinemuri

720 The findings of this study, as well as the work of Beaumont et al (1987), Webster
721 (1995), and Sabti et al. (2000), all confirm that there remains an ongoing,
722 moderate threat to the aquatic ecosystem in the Ohinemuri and Waihou
723 catchments from the legacy of mining activities that occurred between 1875 and
724 1955. There remains a sizeable legacy store of approximately 2,260,000 Mg of
725 mine waste within the Ohinemuri floodplain that may be remobilised and
726 transported through the aquatic ecosystem. With concentrations ranging from
727 200-570 mg kg^{-1} for Pb and 29-73 mg kg^{-1} for As, this equates to approximately
728 62-1800 Mg of Pb and 92-230 Mg of As stored within the Ohinemuri and Waihou
729 floodplains. This contrasts with the effective natural recovery of the Shag River
730 system, in East Otago (Black et al., 2004); where between 1890 and 1946, historic
731 gold mining activities in the catchment discharged at least 85,000 Mg of mine
732 tailings. The Shag River catchment is a steep, bedrock-dominated stream system
733 with little sediment storage capacity, and Black et al. (2004) calculated that floods
734 would have almost completely removed the mine tailings from the catchment
735 within c. 60 yr.

736 Given the present low rates of lateral channel movement in the Ohinemuri (there
737 is no demonstrable difference in the position of the Waihou and Ohinemuri river
738 channels today compared to the map published in the 1910 Commission Report;
739 AJHR, 1910), it is extremely unlikely that natural processes will flush mine-waste
740 deposits from the Ohinemuri valley downstream into the Thames estuary. This
741 could occur however during a major flood that resulted in the breaching of stop
742 banks and avulsion of the river channel in a similar manner to the 1907 event. The
743 identification of significant volumes of contaminated mine waste in the
744 Ohinemuri floodplain within the stop bank corridor does have both local and
745 more general implications for channel and floodplain management in similar

historically contaminated urban, industrial and mining-affected river systems in New Zealand**.** Recent proposals (e.g., Biron et al., 2014; Buffin-Bélanger et al., 2015; Choné and Biron, 2016) to move back and even remove stop banks – so called "freedom corridor" initiatives – to mitigate against increasing flooding resulting from anthropogenic climate change, may need to be rethought in floodplains within or downstream of New Zealand's major cities and industrial areas in order to avoid inadvertently remobilizing contaminated sediment.

6. Conclusions

The 1907 flood event in the Ohinemuri and Waihou river catchments deposited approximately 1.13 M m^3 of gold mining tailings across the floodplain in the vicinity of Paeroa township. While this event was somewhat smaller than the 2014 Mount Polley and 1998 Aznalcollar tailings-dam failures, it was an order of magnitude larger than recent well-publicised tailings-dam failures such as the 1996 South America Porco and 2000 Romanian Baia Mare and Baia Borsa accidents. The flood event and the deposition of the mine waste constituted a significant a significant geomorphological and environmental event, was widely remarked upon at the time, and ultimately prompted the establishment of the 1910 Royal Commission of Inquiry into silting of the Ohinemuri and Waihou rivers. The mine waste deposit from the 1907 flood is easily recognised in cores and floodplain profiles as a dirty yellow-coloured silt. Geochemical analysis of the mine-waste deposit shows concentrations of contaminant metals and metalloids exceed both natural background levels and recommended ISQG values for concentrations of Pb, Zn, Cu, As, Ag, and Hg in aquatic sediments. These concentrations pose a moderate to high risk to the aquatic ecosystem of the

771 Ohinemuri and Waihou catchments. The 1907 mine-waste flood deposit serves as
772 a chronological marker for calculating pre- and post-mining floodplain
773 sedimentation rates, which increased from ~0.2 mm yr^{-1} in the early Holocene, to
774 ~5.5-26.8 mm yr^{-1} following the 1907 flood.

775 Notably, concentrations of contaminant metals and metalloids do not show a
776 downstream trend, contrasting with other studies of mine-waste contamination
777 in floodplains. This variation in the Ohinemuri is interpreted to reflect the
778 catastrophic single event dispersal of the mine-waste contamination. Local-scale
779 geomorphology is a significant influence on the thickness of mine-waste deposits.
780 Mine waste is thickest immediately downstream of the Karangahake Gorge, and
781 on the lower floodplain where the river is constrained by topography. Mean grain
782 size of the mine-waste deposit and the post-mining sedimentation rate both
783 correlate strongly with distance downstream. This reflects a reduction in stream
784 power and the dispersal of sediments across the increasingly broad floodplain in
785 the lower reaches.

786 The contaminated floodplain sediments constitute a potentially significant source
787 of secondary pollution for the aquatic environment. There is a risk that in a large
788 flood of equivalent magnitude to the 1907 event, contaminated mine waste could
789 be eroded by channel expansion and/or river channel avulsion resulting in the
790 remobilisation of contaminant metals and metalloids. As the present estimate of
791 the volume of mine waste stored in the floodplain is derived from historic maps
792 and observations along the contemporary channel edge, future work could focus
793 on investigating the thickness and extent of the mine waste deposit at distance
794 from the channel, particularly on the true-left of the Waihou and Ohinemuri
795 rivers, where the floodplain is largely unconstrained by topography.

Acknowledgements

This project was supported by a Massey University Research Fund award to Clement, Fuller and Macklin. Novakova acknowledges support of research plan no. RVO67985831 of the Institute of Geology AS CR v.v.i. Paul Brewer and Willem Toonen are thanked for their assistance with core preparation and NITON XRF measurements, and Gary Tarbuck is thanked for his help with the geochemical analysis. This paper benefitted from helpful discussions and advice from Mike Roche, and the constructive comments of two anonymous reviewers. Thanks to Waikato Regional Council, who made available contour data which was used to produce the floodplain cross sections.

References

Appendix to the Journal of the House of Representatives (AJHR), 1910. Waihou and Ohinemuri Rivers (report of Commission appointed to inquire into silting of): Together with minutes of evidence and exhibits, C-14. Government Printer, Auckland, NZ.

Appendix to the Journal of the House of Representatives (AJHR), 1921-22. Waihou and Ohinemuri Rivers Commission (Report of), D-6F. Government Printer, Wellington, NZ.

Andrews, E.D., 1987. Longitudinal dispersion of trace metals in the Clark Fork River, Montana. In: Averett R.C., McKnight, D.M. (Eds.), Chemical Quality of Water and the Hydrological Cycle. Lewis Publishers, Inc., Chelsea, pp. 179-211.

819 Australian and New Zealand Environment and Conservation Council (ANZECC) and
820 Agriculture and Resource Management Council of Australia and New Zealand
821 (ARMCANZ), 2000. Australian and New Zealand guidelines for fresh and marine
822 water quality. Volume 1, the guidelines. Australian and New Zealand Environment
823 and Conservation Council (ANZECC) and Agriculture and Resource Management
824 Council of Australia and New Zealand (ARMCANZ), Canberra, AU.

825 Axtmann, E.V., Luoma, S.N., 1991. Large-scale distribution of metal contamination
826 in fine-grained sediments of the Clark River, Montana, USA. Applied
827 Geochemistry 6, 75-88.

828 Balaban, S.-I., Hudson-Edwards, K.A., Miller, J.R., 2015. A GIS-based method for
829 evaluating sediment storage and transport in large mining-affected river systems.
830 Environmental Earth Sciences 74, 4685-4698.

831 Beaumont, H.M., Tunnicliff, J.C., Stevenson, C.D., 1987. Heavy metal survey of
832 Coromandel stream. In: Livingstone, M.E. (Ed.), Preliminary Studies on the Effects
833 of Past Mining on the Aquatic Environment, Coromandel Peninsula. National
834 Water and Soil Conservation Authority, Wellington, NZ, pp. 17-48.

835 Bird, G., Brewer, P.A., Macklin, M.G., Serban, M., Balteanu, D., Driga, B., Sorin, Z.,
836 2008. River system recovery following the Novaţ-Roşu tailings dam failure,
837 Maramureş County, Romania. Applied Geochemistry 23(12), 3498-3518.

838 Bird, G., Macklin, M.G., Brewer, P.A., Nikolova, M., Kotsev, T., Mollov, M., Swain,
839 C., 2010. Dispersal of contaminant metals in the mining-affected Danube and
840 Maritsa drainage basins, Bulgaria, eastern Europe. Water, Air and Soil Pollution
841 206(1-4), 105-127.

842 Biron, P.M., Buffin-Bélanger, T., Larocque, M., Choné, G., Cloutier, C.-A., Ouellet,
843 M.-A., Demers, S., Olsen, T., Desjarlais, C., Eyquem, J., 2014. Freedom space for
844 rivers: a sustainable management approach to enhance river resilience.
845 Environmental Management 54**,** 1056-1073.

846 Black, A., Craw, D., Youngson, J.H., Karubaba, J., 2004. Natural recovery rates of a
847 river system impacted by mine tailing discharge: Shag River, East Otago, New
848 Zealand. Journal of Geochemical Exploration 84, 21-34.

849 Black, A., Trumm, D.A., Lindsay, P., 2005. Impacts of coal mining on water quality
850 and metal mobilisation: case studies from West Coast and Otago. In: Moore, T.A.,
851 Black, A., Centeno, J.A., Harding, J.S., Trumm, D.A. (Eds.), Metal Contaminants in
852 New Zealand: Sources, Treatments, and Effects on Ecology and Human Health.
853 Resolutionz Press, Christchurch, NZ, pp. 247-260.

854 Boseley, C., Mauk, J.L., 2008. Mercury contamination from historic gold mining in
855 the Coromandel, New Zealand. Proceedings of the Australasian Institute of
856 Mining and Metallurgy New Zealand Branch Annual Conference 2008, 23-32.

857 Bradley, S.B., 1984. Flood effects of the transport of heavy metals. International
858 Journal of Environmental Studies 22, 225-230.

859 Bradley, S.B., 1989. Incorporation of metalliferous sediments from historic mining
860 into floodplains. GeoJournal 19, 5-14.

861 Bradley, S.B., Cox, J.J., 1990. The significance of the floodplain to the cycling of
862 metals in the River Derwent catchment, UK. The Science of the Total Environment
863 97/98, 441-454.

864 Brathwaite, R.L., Christie, A.B., 1996. Geology of the Waihi area. Institute of
865 Geological and Nuclear Sciences, Wellington.

Brewer, P.A., Dennis, I.A., Macklin, M.G., 2005. The Use of Geomorphological Mapping and Modelling for Identifying Land Affected by Metal Contamination on River Floodplains. UK Department of the Environment, Fisheries and Rural Affairs (DEFRA) Research and Development Report SP 0525.

Buffin-Bélanger, T., Biron, P. M., Larocque, M., Demers, D., Olsen, T., Choné, G., Ouellet, M.-A., Cloutier, C.-A., Desjarlais, C., Eyquem, J., 2015. Freedom space for rivers: an economically viable river management concept in a changing climate. Geomorphology 251, 137-148.

Choné, G., Biron, P.M., 2016. Assessing the relationship between river mobility and habitat. River Research and Applications 32**,** 528-539.

Byrne, P., Byrne, P., Hudson-Edwards, K.A., Bird, G., Macklin, M.G., Brewer, P.A., Williams, R.D., 2017. Water quality impacts of the 2014 Mount Polley mine tailings spill, British Columbia, Canada. Environmental Science & Technology, in review.

Christie, A.B., Brathwaite, R.L., Rattenbury, M.S., Skinner, D.N.B., 2001. Mineral resource assessment of the Coromandel region, New Zealand. Institute of Geological and Nuclear Sciences, Wellington.

Christie, A.B., Simpson, M.P., Brathwaite, R.L., Mauk, J.L., Simmons, S.F., 2007. Epithermal Au-Ag and related deposits of the Hauraki goldfield, Coromandel Volcanic Zone, New Zealand. Economic Geology 102, 785-816.

Christie, A.B., Brathwaite, R.L., Barker, R.G., Skinner, D.N.B., 2008. Mineral resource assessment of the Thames-Coromandel and Hauraki districts, New Zealand (GNS Science Report 2008/14). GNS Science, Lower Hutt, NZ.

889 Ciszewski, D., 2001. Flood-related changes in heavy metal concentrations within
890 sediments of the Biala Przemsza River. Geomorphology 40, 205-218.

891 Craw, D., Chappell, D.A., 2000. Metal redistribution in historic mine wastes,
892 Coromandel Peninsula, New Zealand. New Zealand Journal of Geology and
893 Geophysics 43, 187-198.

894 de Lisle, J.F., 1967. The climate of the Waikato Basin. Earth Science Journal 1, 2-
895 16.

896 De Vos, W., Ebbing, J., Hindel, R., Schalich, J., Swennen, R., van Keer, I., 1996.
897 Geochemical mapping based on overbank sediments in the heavily industrialised
898 border area of Belgium, Germany and the Netherlands. Journal of Geochemical
899 Exploration 56, 91-104.

900 Dennis, I.A., Macklin, M.G., Coulthard, T.J., Brewer, P.A., 2003. The impact of the
901 October-November 2000 floods on contaminant metal dispersal in the Swale
902 catchment, North Yorkshire, UK. Hydrological Processes 17, 1641-1657.

903 Dennis, I.A., Coulthard, T.J., Brewer, P., Macklin, M.G., 2008. The role of
904 floodplains in attenuating contaminated sediment fluxes in formerly mined
905 drainage basins. Earth Surface Processes and Landforms 45, 453-466.

906 Downey, J.F., 1935. Gold-mines of the Hauraki District, New Zealand. Government
907 Printer, Wellington, NZ.

908 Fuller, I.C., Macklin, M.G., Richardson, J.M., 2015. The geography of the
909 Anthropocene in New Zealand: differential river catchment response to human
910 impact. Geographical Research 53, 255-269.

911 Graf, W.L., 1983. Downstream changes in stream power in the Henry Mountains,
912 Utah. Annals of the Association of American Geographers 73, 373–387.

913 Graf, W.L., 1990. Fluvial dynamics of thorium-230 in the Church Rock event,
914 Puerco River, New Mexico. Annals of the Association of American Geographers
915 80, 327-342.

916 Harding, J., Boothroyd, I., 2004. Impacts of mining. In: Harding, J., Mosley, P.,
917 Pearson, C., Sorrell, B. (Eds.), Freshwaters of New Zealand. New Zealand
918 Hydrological Society and New Zealand Limnological Society, Christchurch, NZ, pp.
919 36.1-36.10.

920 Harding, J., Quinn, J., Hickey, C., 2000. Effects of mining and production forestry.
921 In: Collier, K.J., Winterbourn, M.J. (Eds.), New Zealand Stream Invertebrates:
922 Ecology and Implications for Management. New Zealand Limnological Society,
923 Christchurch, NZ, pp. 230-259.

924 Harding, J.S., 2005. Impacts of metals and mining on stream communities. In:
925 Moore, T.A., Black, A., Centeno, J.A., Harding, J.S., Trumm, D.A. (Eds.), Metal
926 Contaminants in New Zealand: Sources, Treatments, and Effects on Ecology and
927 Human Health. Resolutionz Press, Christchurch, NZ, pp. 343-358.

928 Henderson, J., Bartrum, J.A., 1913. The geology of the Aroha Subdivision, Hauraki,
929 Auckland. John Mackay, Government Printer, Wellington.

930 Horrocks, A.J., Thomas, S.M., Tregurtha, C.S., Beare, M.H., Meenken, E.D., 2010.
931 Implications for dry matter production and nitrogen management as soils develop
932 following 'humping and hollowing' on the West Coast. Proceedings of the New
933 Zealand Grassland Association 72, 103-108.

934 Hudson-Edwards, K.A., Macklin, M.G., Curtis, C.D., Vaughn, D.J., 1998. Chemical
935 remobilization of contaminant metals within floodplain sediments in an incising
936 river system: implications for dating and chemostratigraphy. Earth Surface
937 Processes and Landforms 23, 671-684.

938 Hudson-Edwards, K.A., Schell, C., Macklin, M.G., 1999. Mineralogy and
939 geochemistry of alluvium contaminated by metal mining in the Rio Tinto area,
940 southwest Spain. Applied Geochemistry 14, 1015-1030.

941 Hudson-Edwards, K.A., Macklin, M.G., Miller, J.R., Lechler, P.J., 2001. Sources,
942 distribution and storage of heavy metals in the Rio Pilcomayo, Bolivia. Journal of
943 Geochemical Exploration 72, 229-250.

944 Hudson-Edwards, K.A., Macklin, M.G., Jamieson, H.E., Brewer, P.A., Coulthard, T.J.,
945 Howard, A.J., Turner, J., 2003. The impact of tailings dam spills and clean-up
946 operations on sediment and water quality in river systems: the Ríos Agrio-
947 Guadiamar, Aznalcóllar, Spain. Applied Geochemistry 18, 221-239.

948 James, L.A., 2013. Legacy sediment: definitions and processes of episodically
949 produced anthropogenic sediment. Anthropocene 2, 16-26.

950 Jane, G.T., Green, T.G.A., 1983. Morphology and incidence of landslides in the
951 Kaimai Range, North Island, New Zealand. New Zealand Journal of Geology and
952 Geophysics 26, 71-84.

953 Kossoff, D., Hudson-Edwards, K.A., Dubbin, W.E., Alfredsson, M.A., 2011.
954 Incongruent weathering of Cd and Zn from mine tailings: a column leaching study.
955 Chemical Geology 281, 52-71.

956 Lecce, S.A., 1997. Spatial patterns of historical overbank sedimentation and
957 floodplain evolution, Blue River, Wisconsin. Geomorphology 18, 265–277.

958 Lecce, S.A., Pavlowsky, R.T., 1997. Storage of mining-related zinc in floodplain
959 sediments, Blue River, Wisconsin. Physical Geography 18, 424-439.

960 Lecce, S.A., Pavlowsky, R.T., 2014. Floodplain storage of sediment contaminated
961 by mercury and copper from historic gold mining at Gold Hill, North Carolina,
962 USA. Geomorphology 206, 122-132.

963 Leenaers, H., 1989. The transport of heavy metals during flood events in the
964 polluted River Geul (The Netherlands). Hydrological Processes 3, 325-338.

965 Leigh, D.S., 1997. Mercury-tainted overbank sediment from past gold mining in
966 north Georgia, U.S.A. Environmental Geology 30, 244–251.

967 Lewin, J., Wolfenden, P.J., 1978. The assessment of sediment sources: a field
968 experiment. Earth Surface Processes 3, 171-178.

969 Lewin, J., Macklin, M.G., 1987. Metal mining and floodplain sedimentation in
970 Britain. In: Gardiner, V. (Ed.), International Geomorphology 1986 Part 1. Wiley,
971 Chichester, pp. 1009-1027.

972 Lewin, J., Davies, B.E., Wolfenden, P.J., 1977. Interactions between channel
973 change and historic mining sediments. In: Gregory, K.J. (Ed.), River Channel
974 Changes. Wiley, Chichester, pp. 353-367.

975 Lewin, J., Bradley, S.B., Macklin, M.G., 1983. Historical valley alluviation in mid-
976 Wales. Geological Journal 19, 331-350.

977 Ling, L., 2003. The groundwater regime of the Waihi Basin, North Island, New
978 Zealand. PhD Thesis, The University of Auckland.

979 Livingston, M.E., 1987. Preliminary studies on the effects of past mining on the
980 aquatic environment, Coromandel Peninsula. Water and Soil Directorate, Ministry
981 of Works and Development, Wellington, NZ.

982 Lord, R.A., Morgan, P.A., 2003. Metal contamination of active stream sediments
983 in upper Weardale, Northern Pennine Orefield, UK. Environmental Geochemistry
984 and Health 25, 95-104.
985 Macklin, M.G., 1986. Channel and floodplain metamorphosis in the River Nent,
986 Cumberland. In: M.G. Macklin, Rose, J. (Eds.), Quaternary River Landforms and
987 Sediments in the Northern Pennines. London. British Geomorphological Research
988 Group and Quaternary Research Association, pp. 13-19.
989 Macklin, M.G., 1992. Metal contaminated soils and sediment: a geographical
990 perspective. In: Newson, M.D. (Ed.), Managing the Human Impact on the Natural
991 Environment: Patterns and Processes. Belhaven Press, London, pp. 172-195.

992 Macklin, M.G., 1996. Fluxes and storage of sediment-associated metals in
993 floodplain systems: assessment and river basin management issues at a time of
994 rapid environmental change. In, Anderson, M.G., Walling, D.E., Bates, P. (Eds),
995 Floodplain Processes. Wiley, Chichester, pp. 441-460.

996 Macklin, M.G., Dowsett, R.B., 1989. The chemical and physical speciation of trace
997 metals in fine-grained overbank flood sediments in the Tyne basin, northeast
998 England. Catena 16, 135-151.

999 Macklin, M.G., Klimek, K., 1992. Dispersal, storage, and transformation of metal-
1000 contaminated alluvium in the upper Vistula basin, southwest Poland. Applied
1001 Geography 12, 7-30.

1002 Macklin, M.G., Ridgway, J., Passmore, D.G., Rumsby, B.T., 1994. The use of
1003 overbank sediment for geochemical mapping and contamination assessment:
1004 results from selected English and Welsh floodplains. Applied Geochemistry 9,
1005 689-700.

1006 Macklin, M.G., Brewer, P.A., Coulthard, T.J., Turner, J.N., Bird, G., Hudson-
1007 Edwards, K.A., 2002. The chemical and physical impacts of recent mine tailings
1008 dam failures on river systems: key issues for sustainable catchment management
1009 in former and present metal mining areas. Proceedings of a Seminar on Proposed
1010 EU Directive on Mining Waste. Office of the Deputy Prime Minister, London, pp.
1011 18–24.

1012 Macklin, M.G., Brewer, P.A., Balteanu, D., Coulthard, T.J., Driga, B., Howard, A.J.,
1013 Zaharia, S., 2003. The long term fate and environmental significance of
1014 contaminant metals released by the January and March 2000 mining tailings dam
1015 failures in Maramureş County, upper Tisa Basin, Romania. Applied Geochemistry
1016 18, 241-257.

1017 Macklin, M.G., Brewer, P.A., Hudson-Edwards, K.A., Bird, G., Coulthard, T.J.,
1018 Dennis, I.A., Lechler, P.J., Miller, J.R., and Turner, J.N., 2006. A geomorphological
1019 approach to the management of rivers contaminated by metal mining.
1020 Geomorphology 79, 423-447.

1021 Macklin, M.G., Jones, A.F., Lewin, J., 2010. River response to rapid Holocene
1022 environmental change: evidence and explanation in British catchments.
1023 Quaternary Science Reviews 29, 1555-1576.

1024 Macklin, M.G., Lewin, J., Jones, A.F., 2014. Anthropogenic alluvium: an evidence-
1025 based meta-analysis for the UK Holocene. Anthropocene 6, 26-38.

1026 Magilligan, F.J., 1985. Historical floodplain sedimentation in the Galena River
1027 basin, Wisconsin and Illinois. Annals of the Association of American Geographers
1028 75, 583–594.

1029 Magilligan, F.J., 1992. Thresholds and the spatial variability of flood power during
1030 extreme floods. Geomorphology 5, 373–390.

1031 Marcus, W.A., 1987. Copper dispersion in epithermal stream sediments. Earth
1032 Surface Processes and Landforms 12, 217-228.

1033 Marcus, W.A., Meyer, G.A., Nimmo, D.R., 2001. Geomorphic control of persistent
1034 mine impacts on a Yellowstone Park stream and implications for the recovery of
1035 fluvial systems. Geology 29, 355-358.

1036 Mauk, J.L., Hall, C.M., Chesley, J.T., Barra, F., 2011. Punctuated evolution of the
1037 large epithermal province: the Hauraki goldfield, New Zealand. Economic Geology
1038 106, 921-943.

1039 Maunder, W.J., 1974. Climate and climatic resources of the Waikato Coromandal
1040 King Country region. A.R. Shearer, Government Printer, Wellington.

1041 McArthur, J.M., Banerjee, D.M., Hudson-Edwards, K.A., Mishra, R., Purohit, R.,
1042 Ravenscroft, P., Cronin, A., Howarth, R.J., Chatterjee, A., Talukder, A., Houghton,
1043 S., Chadha, D.K., 2004. Natural organic matter in sedimentary basins and its
1044 relation to arsenic in anoxic ground water: the example of West Bengal and its
1045 worldwide implications. Applied Geochemistry 19, 1255-1293.

1046 McCombie, J., 1897. A retrospect of the Ohinemuri goldfield. New Zealand Mines
1047 Record 1, 33-36.

1048 McCormac, F.G., Hogg, A.G., Blackwell, P.G., Buck, C.E., Higham, T.F.G., Reimer,
1049 P.J., 2004. SHCal04 Southern Hemisphere calibration, 0-11.0 cal kyr BP.
1050 Radiocarbon 46, 1087-1092.

1051 McDowell, R.W., 2008. Phosphorus in humped and hollowed soils of the
1052 Inchbonnie catchment, West Coast, New Zealand: I. Variation with age and
1053 distribution. New Zealand Journal of Agricultural Research 51, 299-306.

1054 Miller, J.R., 1997. The role of fluvial geomorphic processes in the dispersal of
1055 heavy metals from mine sites. Journal of Geochemical Exploration, 58, 101-118.

1056 Miller, J.R., Orbock Miller, S.M., 2007. Contaminated rivers: a geomorphological–
1057 geochemical approach to site assessment and remediation. Springer, The
1058 Netherlands.

1059 Miller, J. et al., 1999. Effects of the 1997 flood on the transport and storage of
1060 sediment and mercury within the Carson River valley, West-Central Nevada. The
1061 Journal of Geology 107, 313-327.

1062 Miller, J.R., Lechler, P.J., Hudson-Edwards, K.A., Macklin, M.G., 2002. Lead
1063 isotopic fingerprinting of heavy metal contamination, Rio Pilcomayo Basin,
1064 Bolivia. Geochemistry: Exploration, Environment, Analysis 2, 225-233.

1065 Moore, J.N., Luoma, S.N., 1990. Hazardous wastes from large-scale metal
1066 extraction: a case study. Environmental Science Technology 24, 1279-1285.

1067 Moore, P., Richie, N., 1996. Coromandel gold: a guide to the historic goldfields of
1068 the Coromandel Peninsula. Dunmore Press, Palmerston North, NZ.

1069 Morgan, O., 1988. Ohinemuri and Waitawheta river gorges. Ohinemuri Regional
1070 History Journal 32, 41-43.

1071 NIWA, 2002. Ohinemuri River, Coromandel. Water Resources Update, 1.

1072 NIWA Historic Weather Event Catalog, April 1981 Waikato Storm. Retrieved from
1073 https://hwe.niwa.co.nz/.

1074 Ohinemuri Gazette, 1910. The Royal Commission. The Ohinemuri Gazette,
1075 Volume XXI, Issue 2648, 3 June 1910, 2.

1076 Pang, L., 1995. Contamination of groundwater in the Te Aroha area by heavy
1077 metals from an abandoned mine. Journal of Hydrology (New Zealand) 33, 17-34.

1078 Passmore, D.G., Macklin, M.G., 1994. Provenance of fine-grained alluvium and
1079 late Holocene land-use change in the Tyne basin, northern England.
1080 Geomorphology 9, 127-142.

1081 Phillips, C., 1986. Excavations of Raupa Pa (N53/37) and Waiwhau Village
1082 (N53/198), Paeroa, New Zealand, in 1984. New Zealand Journal of Archaeology 8,
1083 89-113.

1084 Phillips, C., 2000. Waihou journeys: the archaeology of 400 years of Maori
1085 settlement. Auckland University Press, Auckland.

1086 Rang, M.C., Schouten, C.J., 1989. Evidence for historical metal pollution in
1087 floodplain soils: The Meuse. In: Petts, G.E. (Ed.), Historical change of large alluvial
1088 rivers: Western Europe. John Wiley and Sons, Chichester, pp. 127-142.

1089 Richardson, J.M. et al., 2013. Holocene river behaviour in New Zealand: response
1090 to regional centennial-scale climate forcing. Quaternary Science Reviews 69, 8-27.

1091 Richardson, J.M., Fuller, I.C., Holt, K.A., Litchfield, N.J., Macklin, M.G., 2014. Rapid
1092 post-settlement floodplain accumulation in Northland, New Zealand. Catena 113,
1093 292-305.

1094 Sabti, H., Hossain, M.M., Brooks, R.R., Stewart, R.B., 2000. The current
1095 environmental impact of base-metal mining at the Tui Mine, Te Aroha, New
1096 Zealand. Journal of the Royal Society of New Zealand 30, 197-208.

1097 Salmon, J.H.M., 1963. A history of gold-mining in New Zealand. Government
1098 Printer, Wellington, NZ.

1099 Salomons, W., 1995. Environmental impact of metals derived from mining
1100 activities: processes, predictions, prevention. Journal of Geochemical Exploration
1101 52, 5-23.

1102 Stuiver, M., Braziunas, T.F., 1993. Modelling atmospheric 14C influences and 14C
1103 ages of marine samples to 10,000 BC. Radiocarbon 35, 137-189.

1104 Stuiver, M., Reimer, P.J., 1993. Extended 14C database and revised CALIB
1105 radiocarbon calibration program. Radiocarbon 35, 215-230.

1106 Taylor, M.P.T., Kesterton, R.G.H., 2002. Heavy metal contamination of an arid
1107 river environment: Gruben River, Namibia. Geomorphology 42, 311-327.

1108 Turner, J.N., Macklin, M.G., Jones, A.F., Lewis, H., 2010. New perspectives on
1109 Holocene flooding in Ireland using meta-analysis of fluvial radiocarbon dates.
1110 Catena 82, 183-190.

1111 Walling, D.E. et al., 2003. Storage of sediment-associated nutrients and
1112 contaminants in river channel and floodplain systems. Applied Geochemistry 18,
1113 195-220.

1114 Watton, G., 1995. Taming the Waihou: the story of the Waihou Valley catchment
1115 flood protection and erosion control scheme. Waikato Regional Council,
1116 Hamilton, NZ.

1117 Watton, G., 2006. The flood of all floods. Ohinemuri Regional History Journal 50,
1118 18-24.

1119 Webster, J.G., 1995. Chemical processes affecting trace metal transport in the
1120 Waihou River and estuary, New Zealand. New Zealand Journal of Marine and
1121 Freshwater Research 29, 539-553.

1122 Webster-Brown, J., Craw, D., 2005. Metals derived from gold mining around
1123 historic and modern mines. In: Moore, T.A., Black, A., Centeno, J.A., Harding, J.S.,
1124 Trumm, D.A. (Eds.), Metal Contaminants in New Zealand: Sources, Treatments,
1125 and Effects on Ecology and Human Health. Resolutionz Press, Christchurch, NZ,
1126 pp. 213-230.

1127 Weston, F.W., 1927. Thames goldfields: a history from pre-proclamation times to
1128 1927. Thames, NZ.

1129

1130 **List of figures and tables**

1131 **Figure 1**

1132 Map of the Ohinemuri and Waihou catchments. (A) New Zealand context map. (B)
1133 Map of the Waihou River catchment. (C) Map of the Ohinemuri River catchment
1134 showing the location of tributary rivers, towns, mine workings, and stamper
1135 batteries. Locations of mine workings and stamper batteries after Moore and
1136 Richie (1996).

1137 **Figure 2**

1138 Photo of a ‘silt-bank’ at Pereniki Bend (see Fig. 4) on the outskirts of Paeroa
1139 township, taken in June 1907. The Ohinemuri River channel was formerly

adjacent to the willow tree on the left of the image, and settlers used to tie their boats to the willow tree in about 6 ft of water. The silt is described as a dirty, yellow-brown talcum-like silt (AJHR, 1910). Photo from AJHR (1910).

Figure 3

Photo taken in June 1907 of Wairere Paddocks, in the vicinity of Mackaytown (see Fig. 2), destroyed by silt deposited by the January 1907 flood. The silt is described as talcum-like and dirty, yellow-brown in colour. (See Fig. 8 for examples of the contemporary appearance of the mine-waste flood deposit in section.) View is looking upstream, with the Ohinemuri River behind the willow trees on the left of the photo. Photo from AJHR (1910).

Figure 4

Map of the study area around the township of Paeroa and the Ohinemuri-Waihou confluence. Shown are the locations of cores G and M, floodplain sections Oh-1 to Oh-5 and Wai-1 to Wai-4, and bulk sediment samples recovered from the Ohinemuri River channel (Ke-1 to Ke-3; see inset map for location of Ke-4) and the Ohinemuri River bank (Wi-1, see inset map for location). The documented passage of the 1907 flood is indicated (the ‘zone of overflow’, marked as such in maps in AJHR, 1910), as is the thickness of post-flood silt deposits mapped as part of the 1910 inquiry (AJHR, 1910). Post-1910 cuts to the Waihou channel and the realignment of the Ohinemuri channel are also shown. Flow of both the Waihou and Ohinemuri rivers is from south to north.

Figure 5

Stratigraphy, sedimentology, and geochemistry results for core G. Geochemical concentrations were analysed using a NITON hand-held XRF scanner. Vertical green lines show the ISQG-low concentrations for Pb, Zn, and As.

Figure 6

Stratigraphy, sedimentology, and geochemistry results for core M. Pb, Zn, Fe, As, and Cu expressed in mg kg^{-1}were analysed using a NITON hand-held XRF scanner. The layer interpreted to be the 1907 mine-waste flood deposit is shown in yellow. Vertical green and red lines show the ISQG-low (green) and ISQG-high (red) concentrations for Pb, Zn, As, and Cu.

Figure 7

Stratigraphy, sedimentology, and geochemistry results for floodplain profiles Oh-1 to Oh-5. The locations of these sections are shown on Fig. 5. Concentrations of Pb, As, Zn, Cu and Fe were determined using ICP-OES.

Figure 8

Photos of the mine-waste deposit from the 1907 flood in sections (a) Oh-1; (b) Oh-2; and (c) Oh-4. The top and bottom of the mine-waste unit in each section is indicated with arrows. Note the distinctive yellow colouring of the mine waste (cf. AJHR, 1910).

Figure 9

Stratigraphy, sedimentology, and geochemistry results for floodplain profiles Wai-1 to Wai-4. The locations of these sections are shown on Fig. 5. Concentrations of Pb, As, Zn, Cu and Fe were determined using ICP-OES.

Figure 10

Photo of reduced mine waste (grey sand) at the base of floodplain section Oh-5.

Figure 11

Characterisation of the floodplain topography of the Ohinemuri and Waihou rivers, expressed as cross sections taken at each of the sampling sites down the length of the river. (A) Map of the study area, showing the location of cross sections. Cross sections 1 to 7 correspond to the numbered lines on this map. The left of each cross section corresponds with the true-left of the floodplain. Flow of both rivers is from south to north. Elevation data for the cross sections is derived from contour data made available by Waikato Regional Council.

Figure 12

Downstream trends in: (A) concentrations of Pb, As, and Cu in mine-waste flood deposits; (B) the thickness of the mine waste flood deposits; (C) the mean grain size of the mine-waste flood deposits; and (D) the post-1907 sedimentation rate.

Table 1

Summary of the geochemical analyses performed on each of the sedimentary samples presented in the current study.

Table 2

Results of radiocarbon age determinations of organic material recovered in cores G and M.

Table 3

Geochemical results from bulk sediment samples Ke-1 to -4 and Wi-1. Concentrations of As, Ag, Hg and Pb, were measured using ICP MS, concentrations of Cu and Zn were determined using AAS.

Table 4

Volumes of mine waste estimated for the Ohinemuri River valley. Polygons (areas where mine waste was deposited) were derived from maps presented in AJHR (1910); polygon numbers correspond to labels on Supp. Fig. 1. Mine waste thickness at the channel edge is derived from observations of this study (see Figs. 7 and 9). The sum of the final column is 1,129,332 m^3 of mine waste.

Table 5

Recommended interim guidelines (ISQG) for concentrations of contaminant metals and metalloids for aquatic sediments in New Zealand. From ANZECC and ARMCANZ (2000).

Table 6

Average concentrations and ranges (in brackets) of As, Cu, Pb, and Zn in mining-affected floodplains in New Zealand (Ohinemuri, this study) and internationally.

Supplementary Figure 1

Map of the study area around the township of Paeroa and the Ohinemuri-Waihou confluence. Shown is the area of silt coverage mapped in 1910. The area downstream between Wai-3 and Wai-4 has been extended as mine waste was located at Wai-4 (cf. Fig. 5). The area of mine waste has also been extended upstream of Oh-2 as mine was located at Oh-1. Descriptions of the mine waste thickness are taken from AHJR (1910). Numbers in italics are the thicknesses of

mine waste used for calculating the legacy volume of mine waste present in the floodplain. Numbers in brackets are polygon numbers in the range 1-18 used to estimate the volume of mine waste presently stored in the floodplain, and correspond with polygon numbers presented in Table 4.

Supplementary Table 1

Results of correlation of Niton XRF results of As, Pb with results from ICP MS analysis, and correlations of Cu and Zn concentrations from Niton XRF with results of Cu and Zn measured by AAS.

Table 1

Table 1: Summary of the geochemical analyses performed on each of the sedimentary samples presented in the current study.

Sample	Type of sediments	Analysed elements	Instrument
M, G	Percussion cores from floodplains	As, Cu, Fe, Pb, Zn	Handheld XRF Niton Aberystwyth University
Oh-1 to -5 Wai-1 to -4	Bulk samples from floodplain profiles in exposed riverbanks	As, Cu, Fe, Pb, Zn	ICP-OES University of London
Wi-1 Ke-1 to -4	Bulk sediments from overbank and channel sediments	Ag, As, Hg, Pb	ICP-MS Aberystwyth University
		Cu, Zn	AAS Aberystwyth University

Table 2

Table 2: Results of radiocarbon age determinations of organic material recovered in cores G and M.

Core	Depth (m)	Material dated	Lab number	Conventional radiocarbon age (yr BP)	2-σ Sidereal age (cal BP)
G	1.0	Wood	Wk-39424	5178±26	5870±120
M	1.6	Rootlets	Wk-39428	7940±30	8790±190

Table 3

Table 3: Geochemical results from bulk sediment samples Ke-1 to Ke-4 and Wi-1. Concentrations of As, Ag, Hg and Pb, were measured using ICP MS, concentrations of Cu and Zn were determined using AAS.

Sample	Sample type	Pb (mg kg^{-1})	Zn (mg kg^{-1})	As (mg kg^{-1})	Cu (mg kg^{-1})	Hg (mg kg^{-1})	Ag (mg kg^{-1})
Ke-1	Channel sediment	34	69	20	24	0.44	0.40
Ke-2	Channel sediment	29	56	40	23	0.45	0.33
Ke-3	Channel sediment	111	138	29	31	0.50	2.93
Ke-4	Channel sediment	20	68	25	22	0.33	0.35
Wi-1	Overbank silts	104	323	16	24	0.44	2.51

Table 4

Table 4: Volumes of mine waste estimated for the Ohinemuri River valley. Polygons (areas where mine waste was deposited) were derived from maps presented in AJHR (1910); polygon numbers correspond to labels on Supp. Fig. 1. Mine waste thickness at the channel edge is derived from observations of this study (see Figs. 7 and 9). The sum of the final column is 1,129,332 m^3 of mine waste.

Polygon	Area (m^2)	Description of mine-waste deposit from AJHR (1910)	Thickness of mine waste at channel edge (m)	Source of mine waste thickness estimate	Maximum calculated volume of mine waste (area × thickness), assuming no decrease in thickness with distance from the channel (m^3)	Calculated volume of mine waste, assuming thickness decreases to 30% at distal margin of polygon ([area × thickness] × 0.65)
1	10,487	-	0.20	Oh-1	2097	1363
2	74,047	-	0.20	Oh-1	14,809	9626
3	41,692	-	0.20	Oh-1	8338	5420
4	55,679	-	0.50	Oh-2	27,839	18,095
5	655,680	Heavy	0.50	Oh-2	327,840	213,096
6	590,176	Heavy	0.50	Oh-2	295,088	191,807
7	43,624	-	0.18	Core M	7852	5104
8	25,790	-	0.18	Core M	4642	3017
9	474,510	Heavy	0.30	Described as a 'heavy silt deposit'; presumed to be an intermediate thickness between Core M and Oh-2	142,353	92,529
10	410,583	-	0.18	Core M	73,905	48,038
11	2,165,751	Light	0.18	Core M	389,835	253,393
12	56,050	-	0.22	Oh-3	12,331	8015
13	118,924	-	0.50	Oh-5	59,462	38,650
14	661,624	Light	0.15	Described as a 'light silt deposit', presumed to be similar thickness to Core M and Wai-4	99,244	64,509
15	254,472	Heavy	0.50	Oh-5	127,236	82,703
16	293,703	-	0.15	Wai-4	44,056	28,636
17	439,325	-	0.15	Described as a 'light silt deposit', presumed to be similar thickness to Core M and Wai-4	65,899	42,834
18	230,743	-	0.15	Wai-4	34,611	22,497

Table 5: Recommended interim sediment quality guidelines (ISQG) for concentrations of contaminant metals and metalloids for aquatic sediments in New Zealand. From ANZECC and ARMCANZ (2000).

Contaminant	ISQG-low trigger value (mg kg^{-1} dry wt)	ISQG-high trigger value (mg kg^{-1} dry wt)
Pb	50.00	220.00
Zn	200.00	410.00
Cu	65.00	270.00
Cr	80.00	370.00
Ni	21.00	52.00
Cd	1.50	10.00
Sb	2.00	25.00
Ag	1.00	3.70
Hg	0.15	1.00
As	20.00	70.00

Table 6

Table 46: Average concentrations and ranges (in brackets) of As, Cu, Pb, and Zn in mining-affected floodplains in New Zealand (Ohinemuri, this study) and internationally.

Area	As (mg/kg)	Cu (mg/kg)	Pb (mg/kg)	Zn (mg/kg)
Ohinemuri (this study) (n=34)	30 (2-73)	43 (18-130)	230 (47-570)	140 (30-910)
Upper Río Pilcomayo, Bolivia (n=7)[a]	2500 (210-7200)	490 (88-1400)	960 (230-1700)	8200 (1800-10000)
Mining- and industrially-contaminated sites in Belgium, Germany and the Netherlands (n=34)[b]	16 (<5-69)	25 (<10-736)	89 (<10-1600)	716 (378-2477)
River Someş, Romania (n=8)[c]	102 (9-300)	110 (11-880)	439 (18-2760)	368 (54-9200)
Aznalcóllar, Spain (n=93)[d]	(27-1200)	(17-730)	(50-2700)	(140-4600)
Río Tinto, Spain (n=14)[e]	370 (110-750)	300 (75-1500)	2800 (490-3100)	200 (<20-120)
River Nent, UK (n=24)[f]	nr	nr	5262 (224-15800)	16320 (4360-38000)
River Swale, UK (n=297)[g]	nr	nr	(75-8052)	(50-3885)
River Wear, UK (n=107)[h]	(<10-65)	(<10-340)	20-15000	40-1500
River Ystwyth, UK (n=41)[i]	nr	nr	1791 (73-4646)	533 (123-1543)

nr: not reported; [a] Hudson-Edwards et al., 2001; [b] De Vos et al., 1996; [c] Macklin et al., 2003; [d] Hudson-Edwards et al., 2003; [e] Hudson-Edwards et al., 1999; [f] Macklin, 1986; [g] Brewer et al., 2005; [h] Lord and Morgan, 2003; [i] Lewin et al., 1983.

Supplementary Table 1

Supplementary Table 1: Results of correlation of Niton XRF results of As, Pb with results from ICP MS analysis, and correlations of Cu and Zn concentrations from Niton XRF with results of Cu and Zn measured by AAS.

Measurmeent comparison	Measured element	Correlation equations	Number of samples	r^2
XRF with ICP MS	As	y = 1.0102x	11	0.966
	Pb	y = 1.2309x	11	0.996
XRF with AAS	Cu	y = 0.102x + 32.73	8	0.402
	Zn	y = 0.8424x	10	0.705

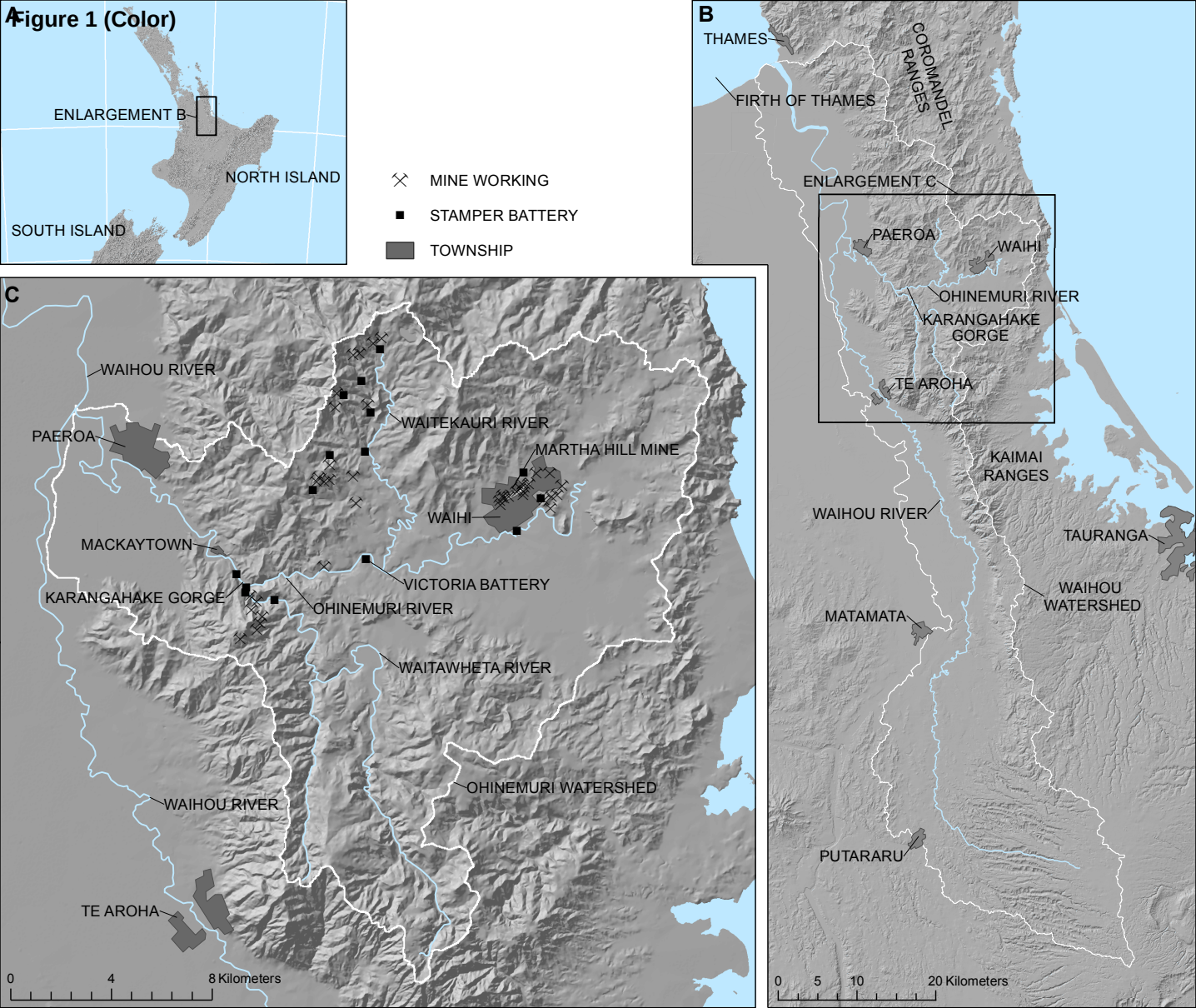
Figure 1 (Color)
A
ENLARGEMENT B
NORTH ISLAND
SOUTH ISLAND
MINE WORKING
STAMPER BATTERY
TOWNSHIP
B
THAMES
FIRTH OF THAMES
CORMANDEL RANGES
ENLARGEMENT C
PAEROA
WAIHI
OHINEMURI RIVER
KARANGAHAKE GORGE
TE AROHA
KAIMAI RANGES
WAIHOU RIVER
TAURANGA
WAIHOU WATERSHED
MATAMATA
PUTARARU
0 5 10 20 Kilometers
C
WAIHOU RIVER
PAEROA
WAITEKAURI RIVER
MARTHA HILL MINE
WAIHI
MACKAYTOWN
VICTORIA BATTERY
KARANGAHAKE GORGE
OHINEMURI RIVER
WAITAWHETA RIVER
OHINEMURI WATERSHED
WAIHOU RIVER
TE AROHA
0 4 8 Kilometers

Figure 2 (Color)

Figure 3 (Color)

Figure 4 (Color)

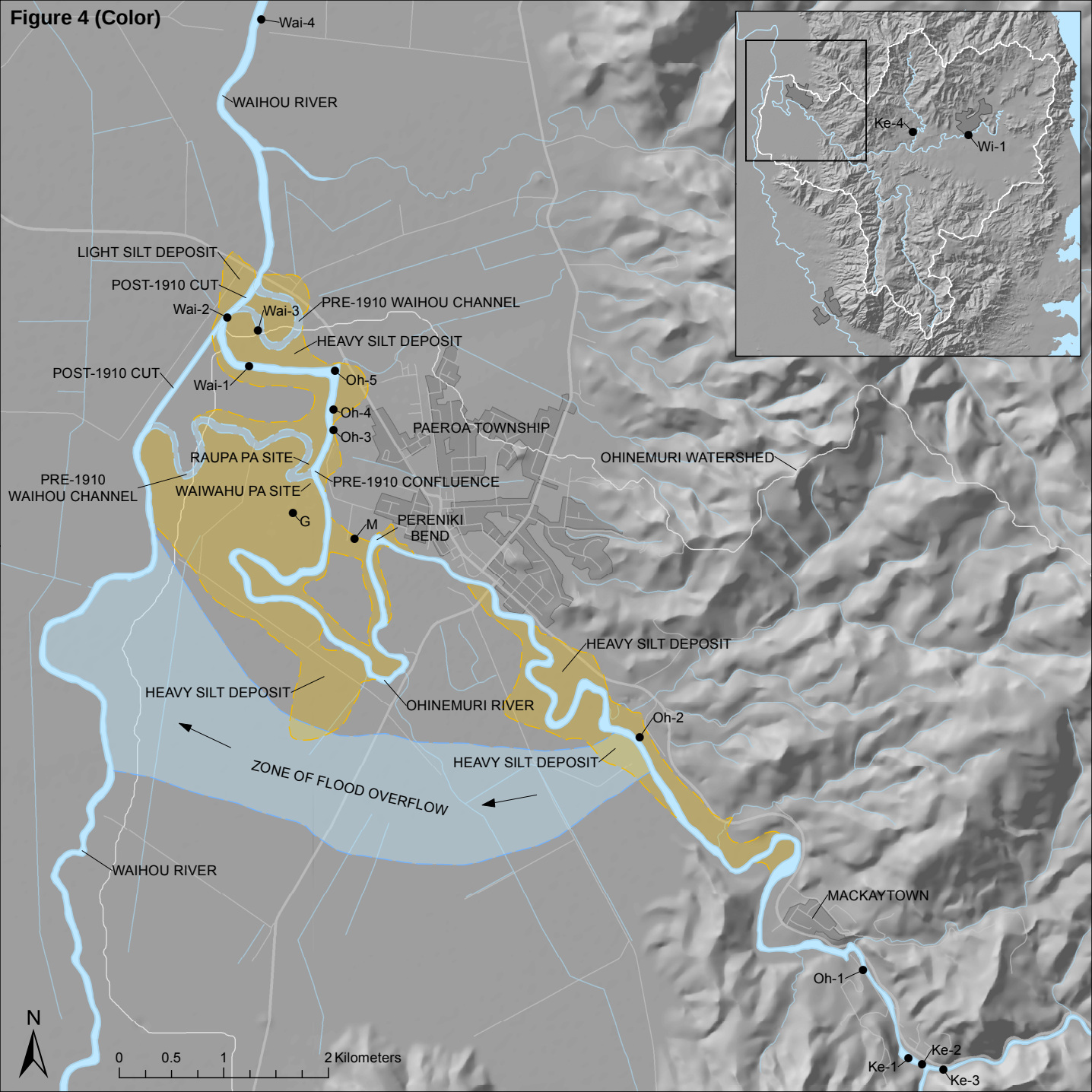

Figure 5 (Color)

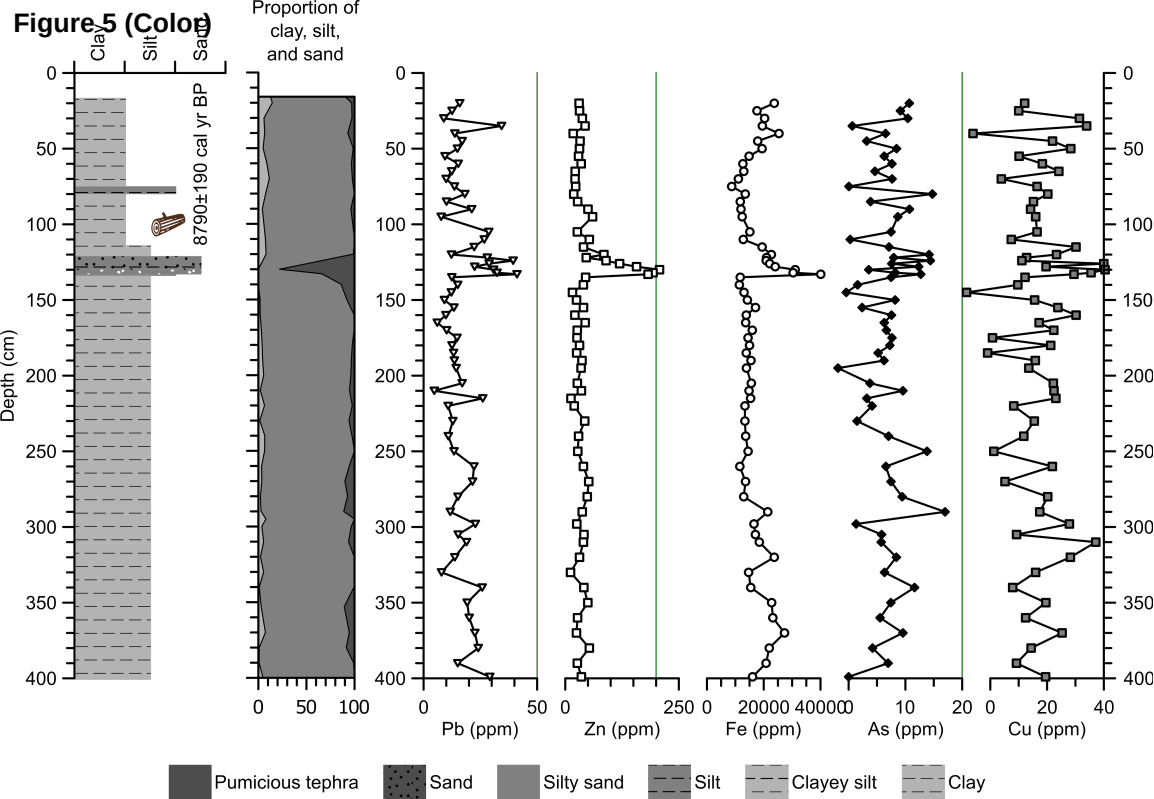

Figure 6 (Color)

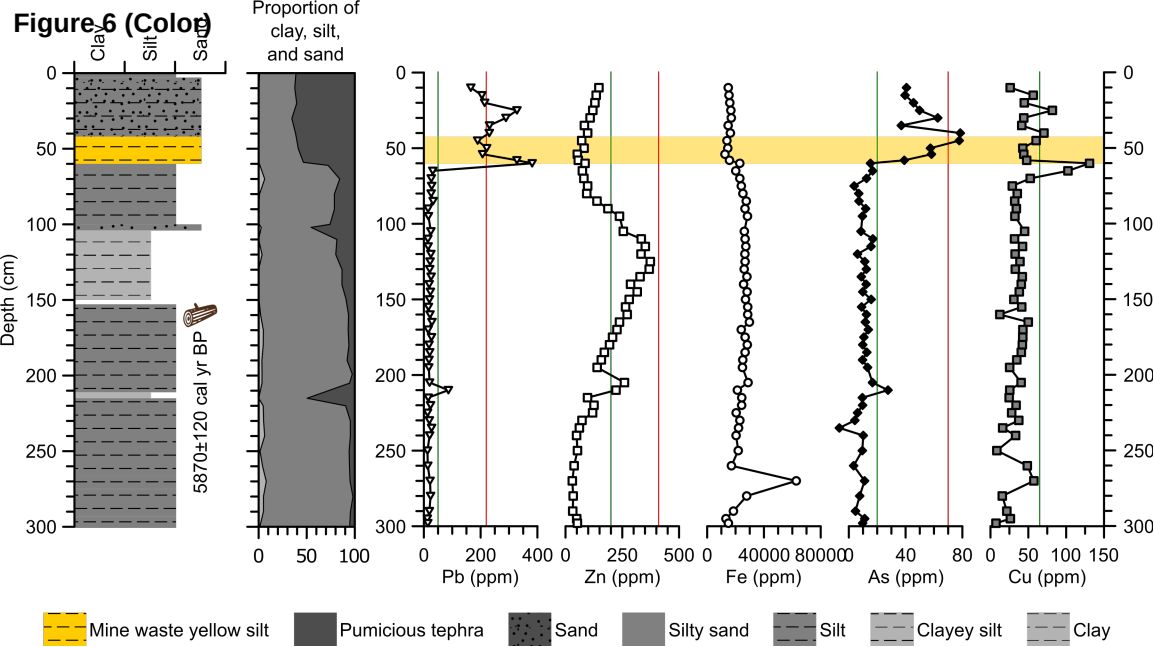

Figure 7 (Color)

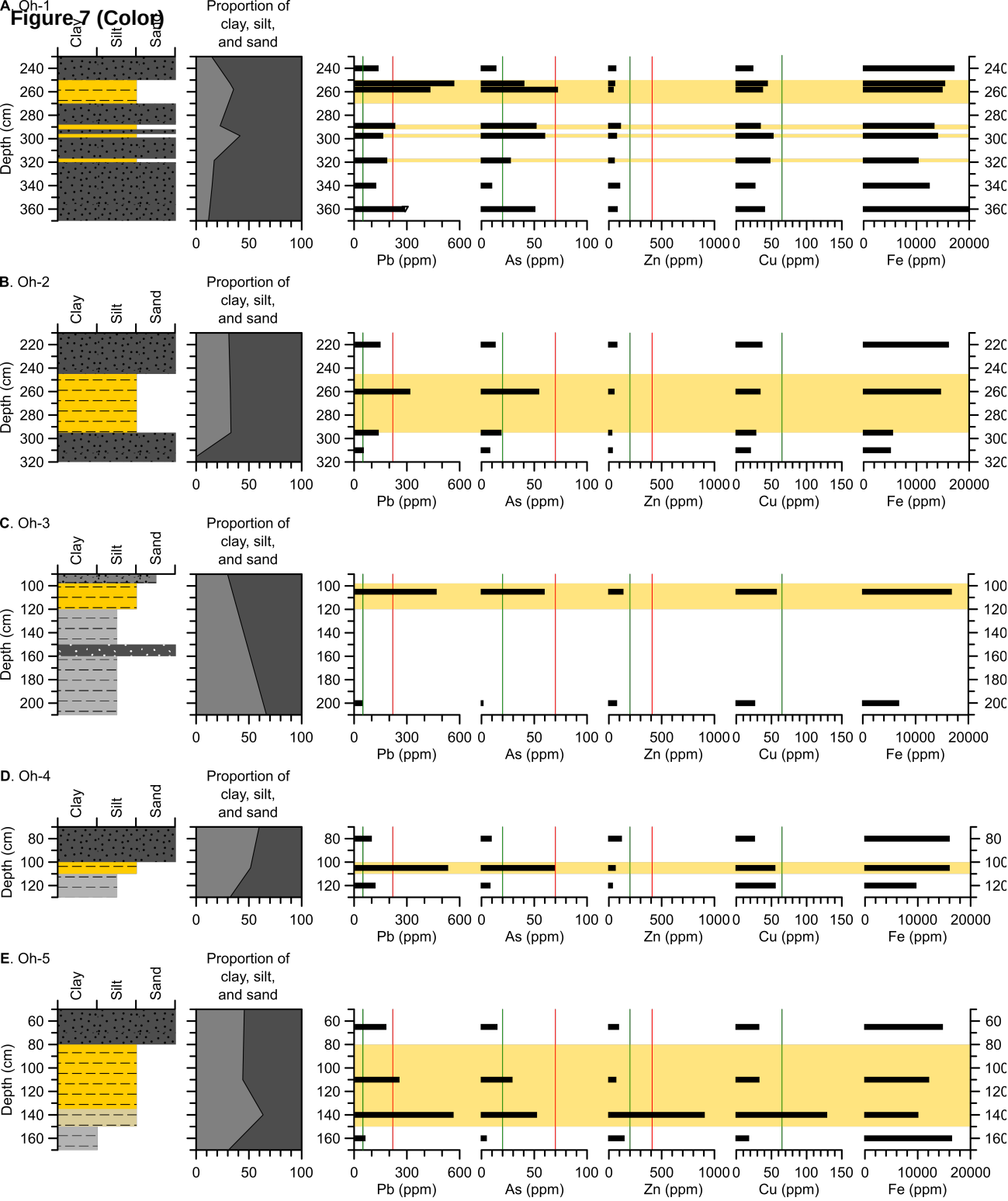

Figure 8 (Color)

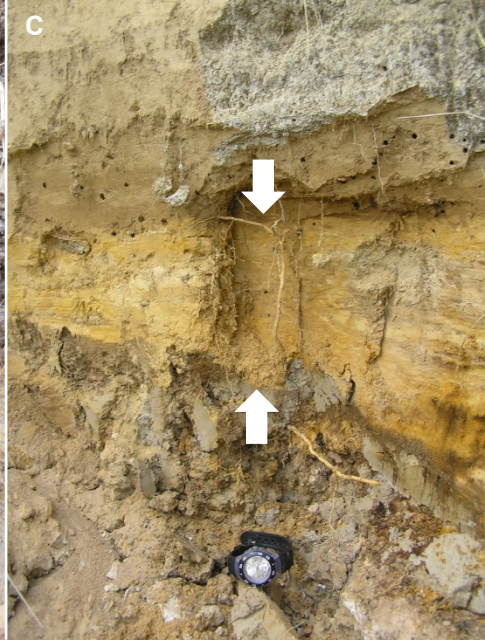

Figure 9 (Color)

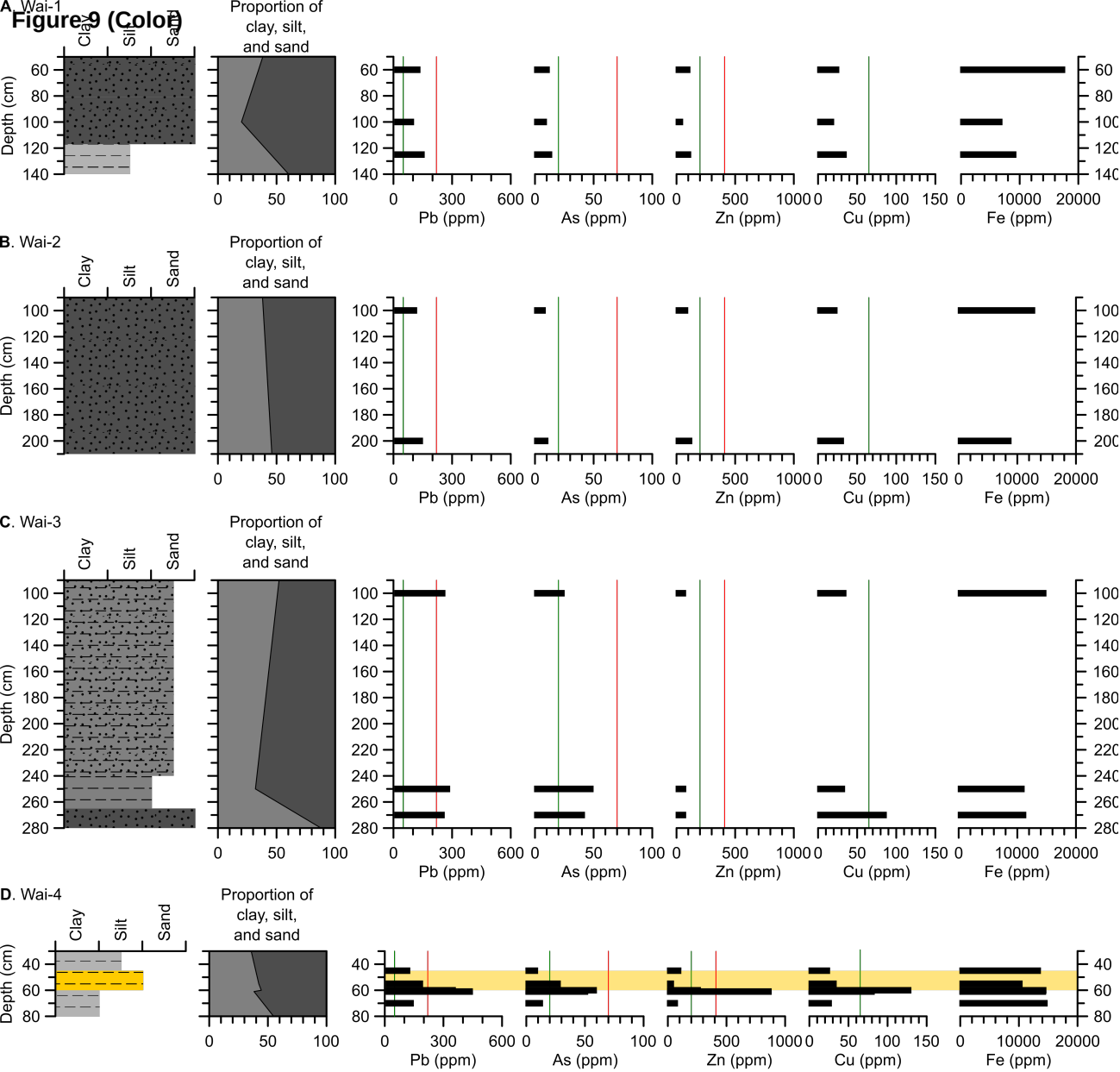

Figure 10 (Color)

Figure 11 (Color)

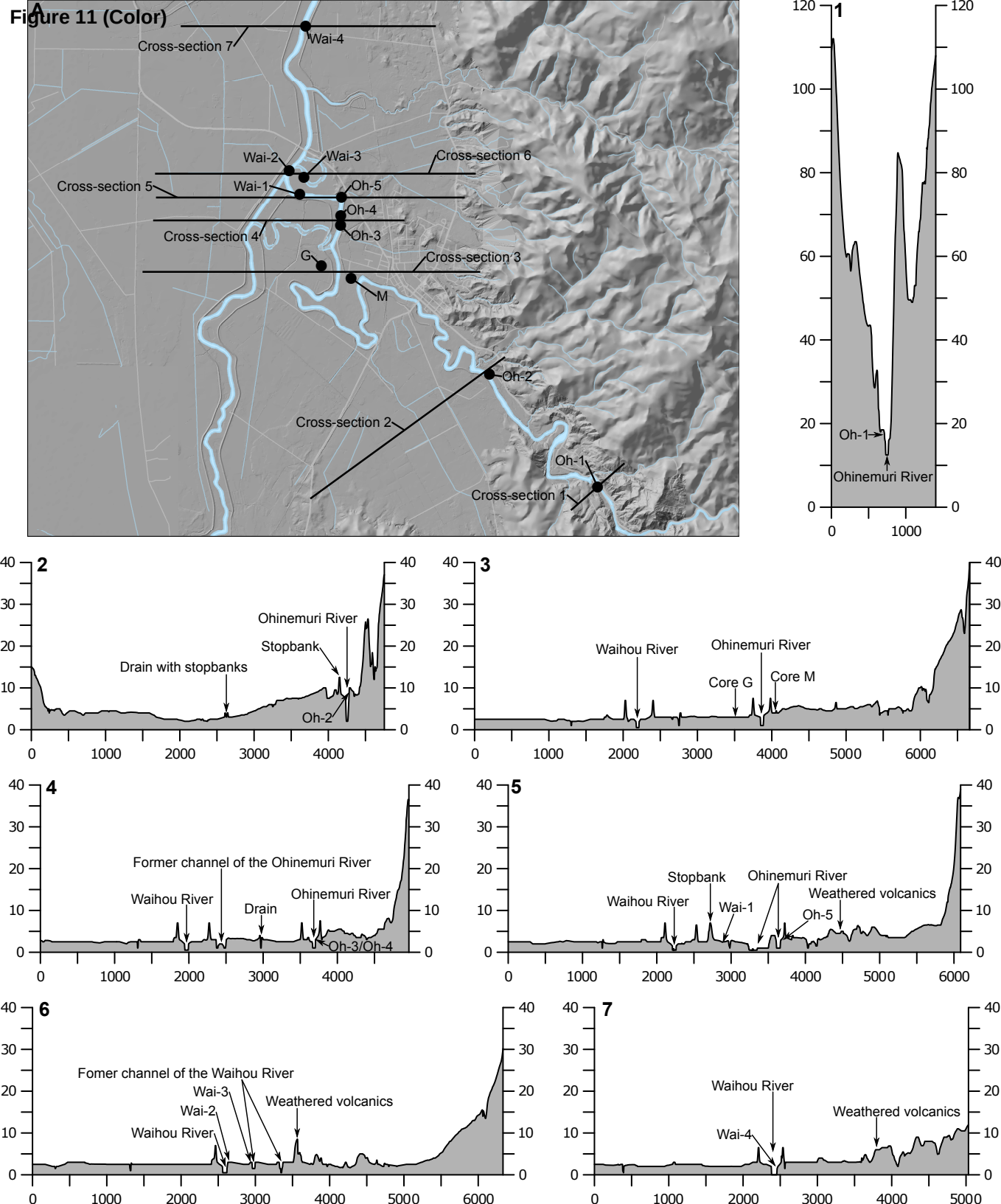

Figure 12 (Color)

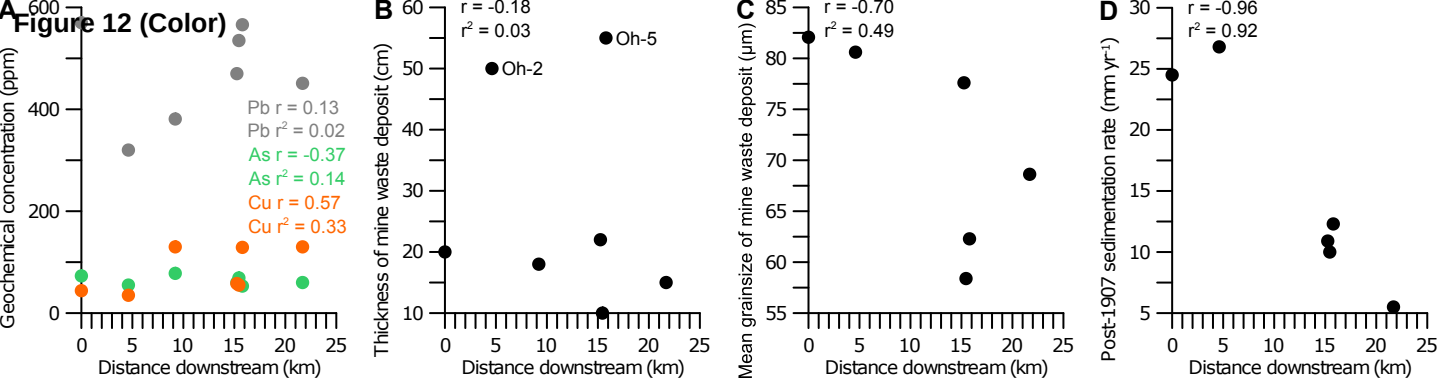

Supplementary Figure 1 (Color)